

Study of Defects in GaN by Positron Annihilation

R. Krause-Rehberg

Univ. Halle



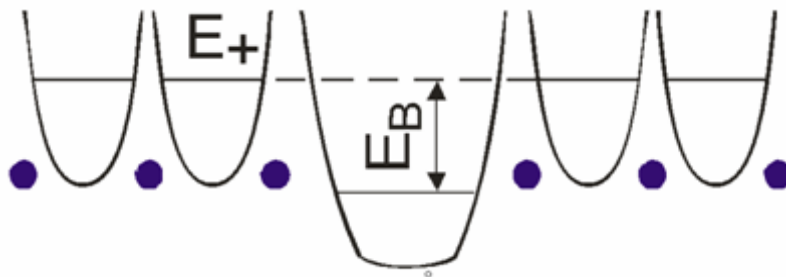
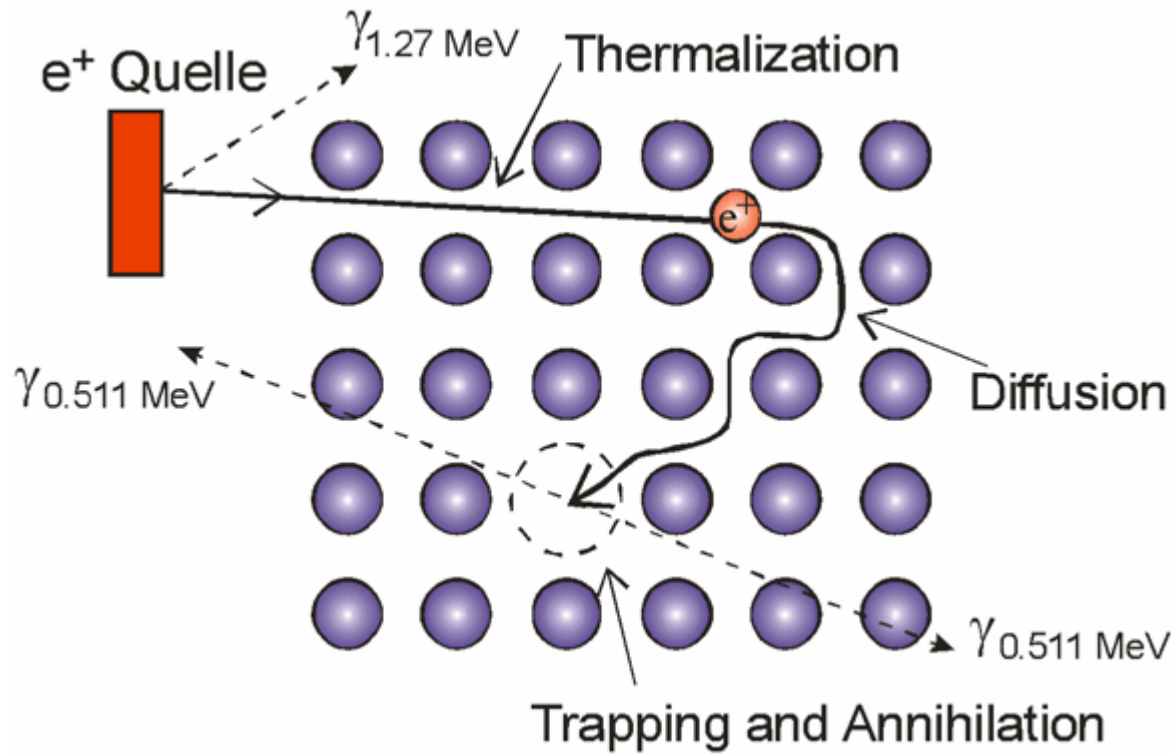
Martin-Luther-Universität
Halle-Wittenberg

- The method:
 - positron lifetime spectroscopy
 - Coincidence Doppler broadening spectroscopy
 - positron beam technique - the MePS system at ELBE at HZDR
- GaN results



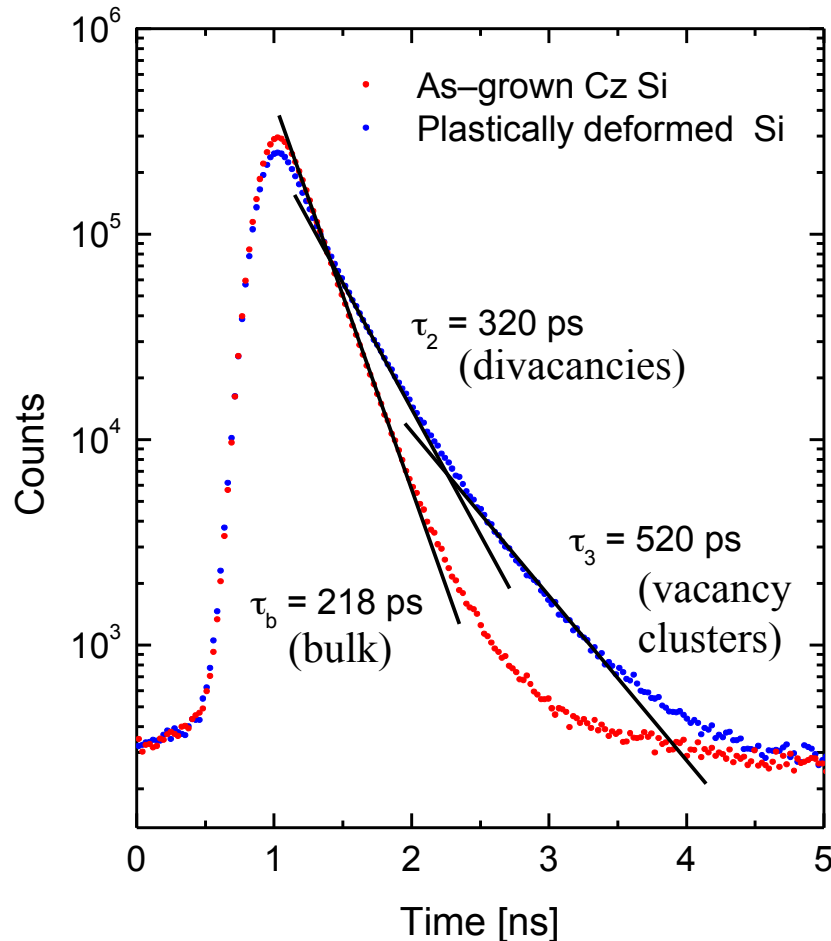
The positron lifetime spectroscopy

^{22}Na



- positron wave-function can be localized in the attractive potential of a defect
- annihilation parameters change in the localized state
- e.g. positron lifetime increases in a vacancy
- lifetime is measured as time difference between appearance of 1.27 (start) and 0.51 MeV (stop) quanta
- defect identification and quantification possible

Positron lifetime spectroscopy



- positron lifetime spectra consist of exponential decay components
- positron trapping in open-volume defects leads to long-lived components
- longer lifetime due to lower electron density
- analysis by non-linear fitting: lifetimes τ_i and intensities I_i

positron lifetime spectrum:

$$N(t) = \sum_{i=1}^{k+1} \frac{I_i}{\tau_i} \exp\left(-\frac{t}{\tau_i}\right)$$

trapping coefficient

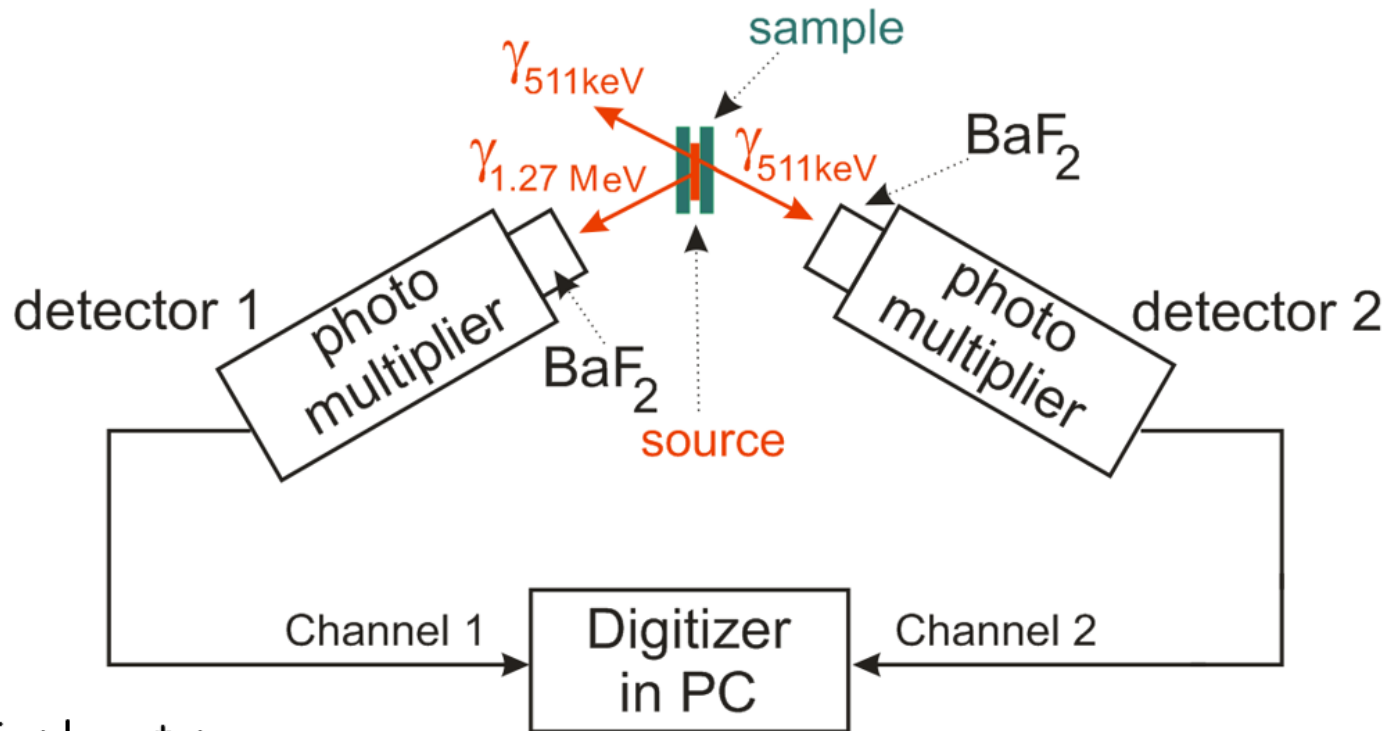
$$k_d = \mu C_d = \frac{I_2}{I_1} \left(\frac{1}{\tau_b} - \frac{1}{\tau_d} \right)$$

trapping rate

defect concentration

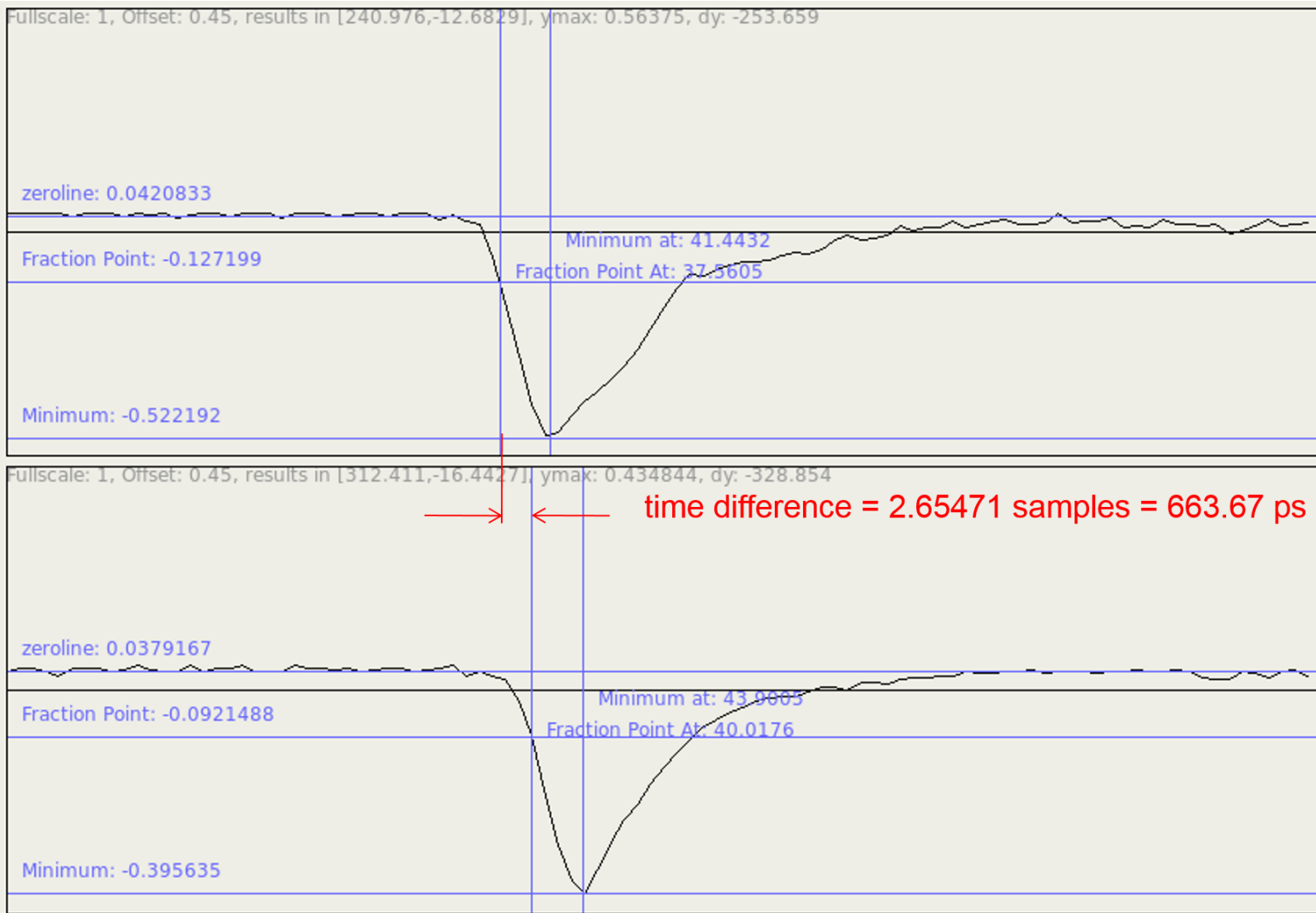


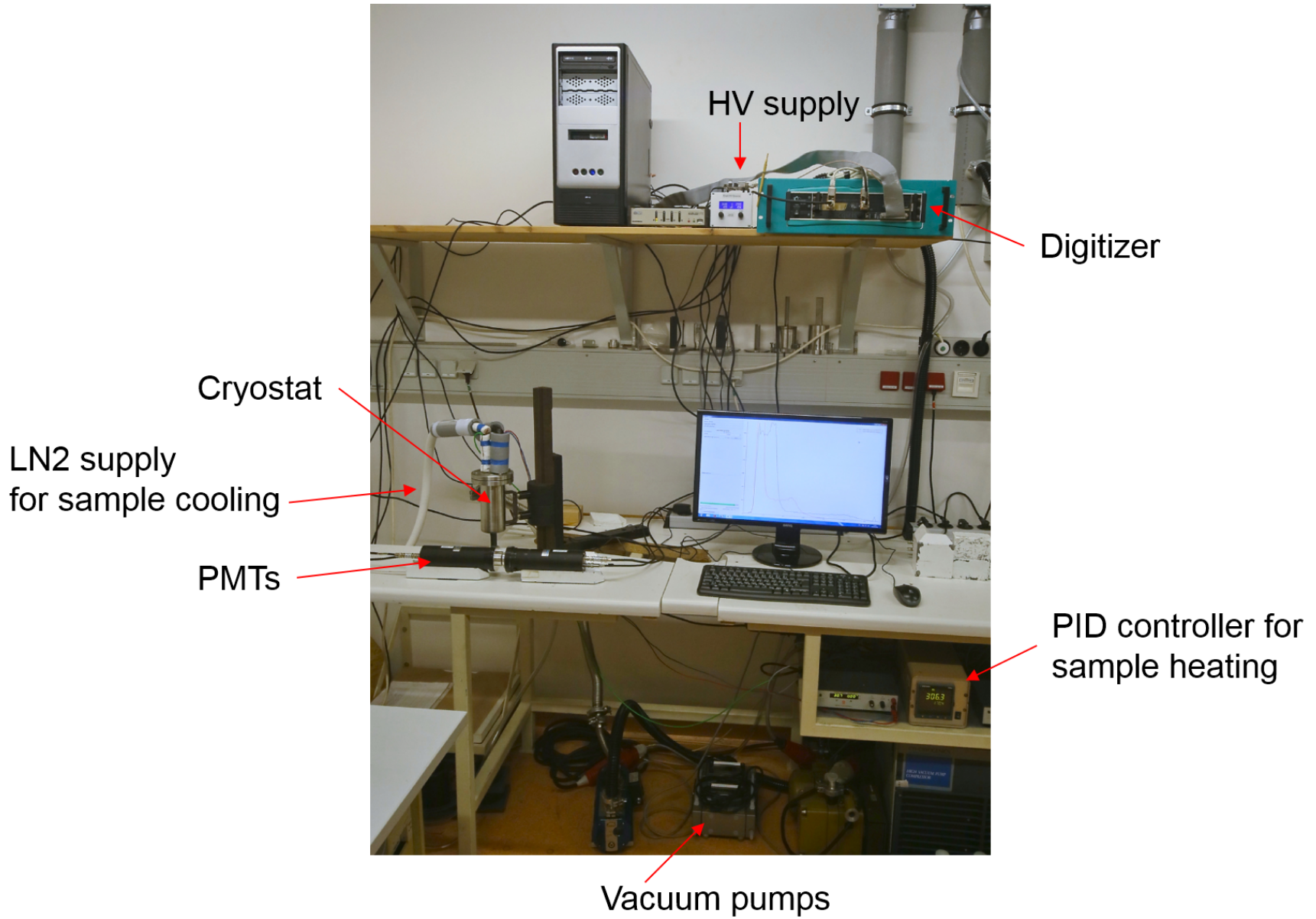
Digital positron lifetime measurement



- simple setup
- timing very accurate
- each detector for start & stop (double statistics)

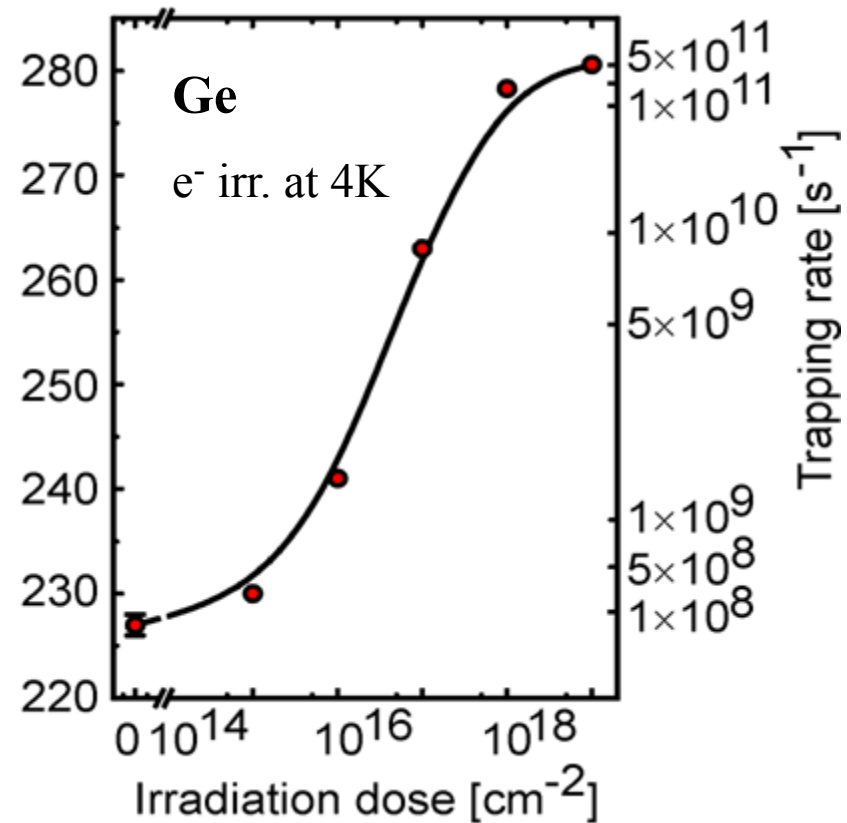
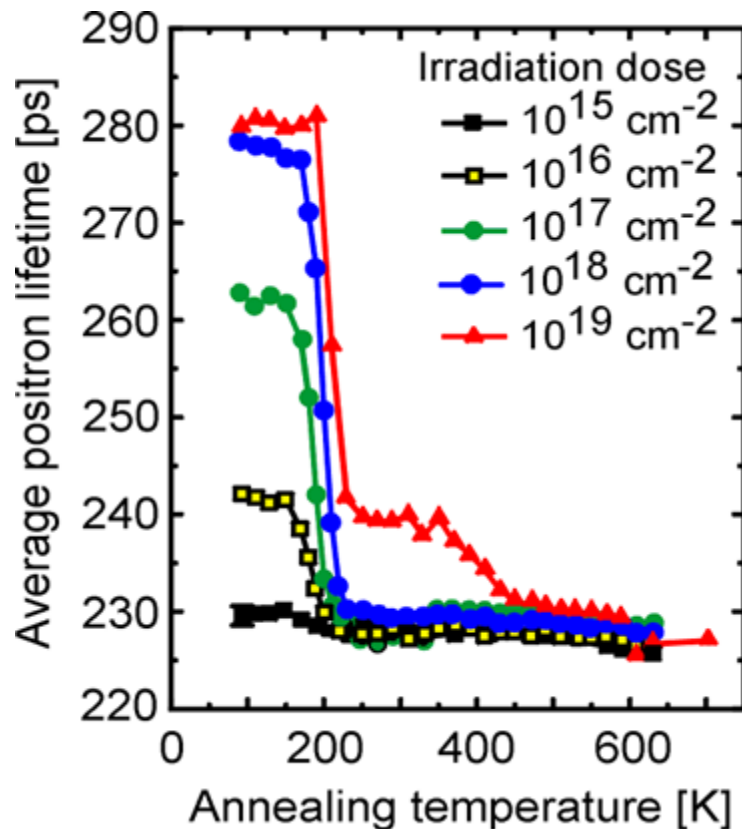
Digital positron lifetime measurement





Defects in electron-irradiated Ge

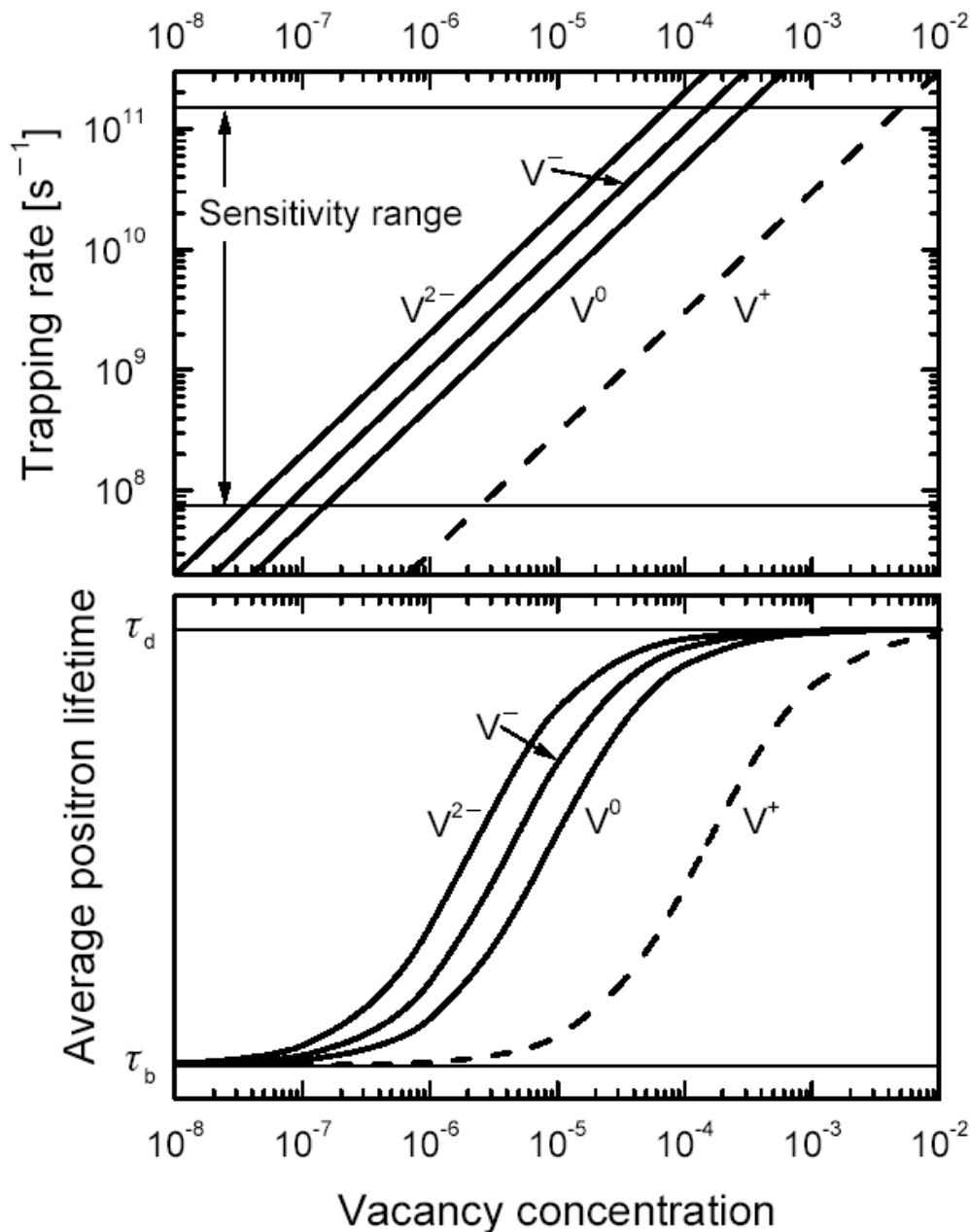
- Electron irradiation (2 MeV @ 4K) induces Frenkel pairs (vacancy - interstitial pairs)
- steep annealing stage at 200 K
- at high irradiation dose: divacancies are formed (thermally more stable)



(Polity et al., 1997)

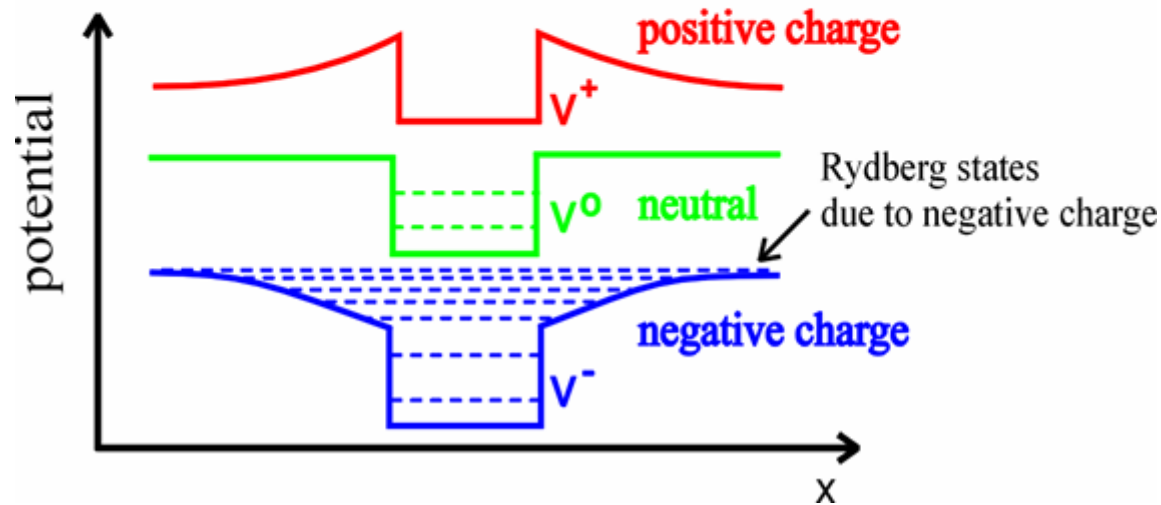
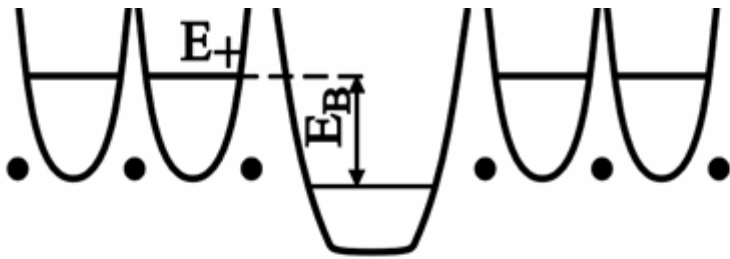


Sensitivity limits of PAS for vacancy detection



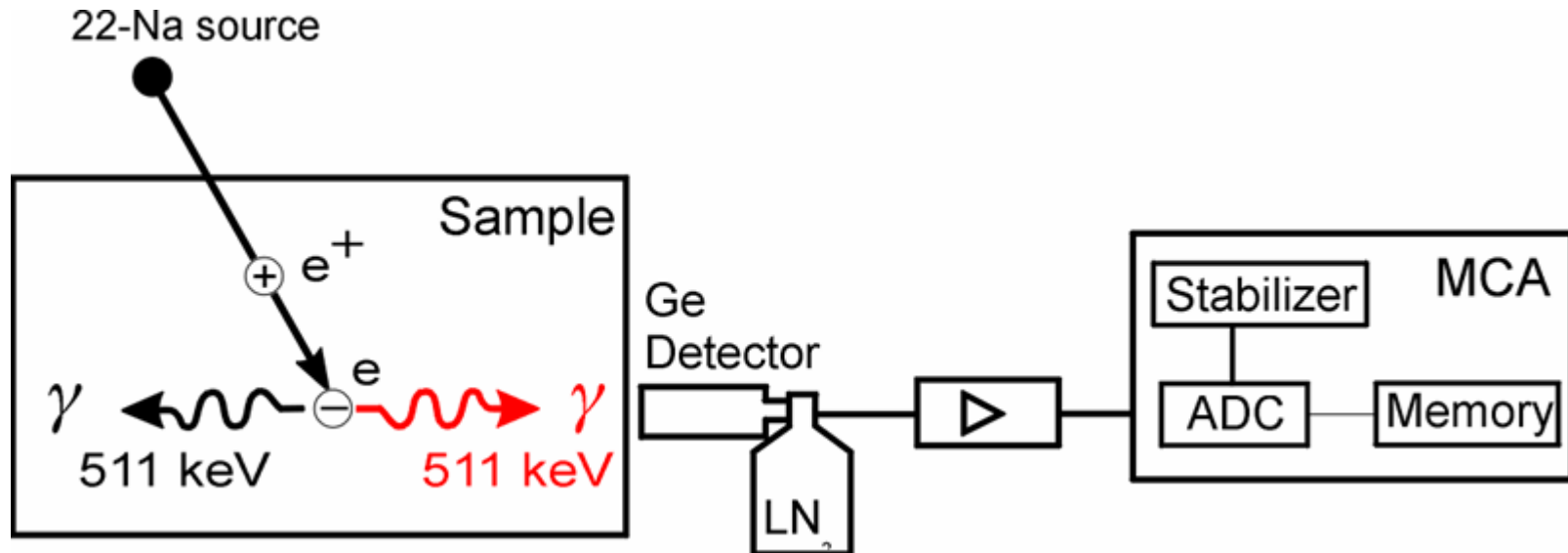
- **lower sensitivity limit** e.g. for negatively charged divacancies in Si starts at about 10^{15} cm^{-3}
- **upper limit**: saturated positron trapping
- defect identification still possible
- Then: only lower limit for defect density can be given

Vacancies in a semiconductor may be charged



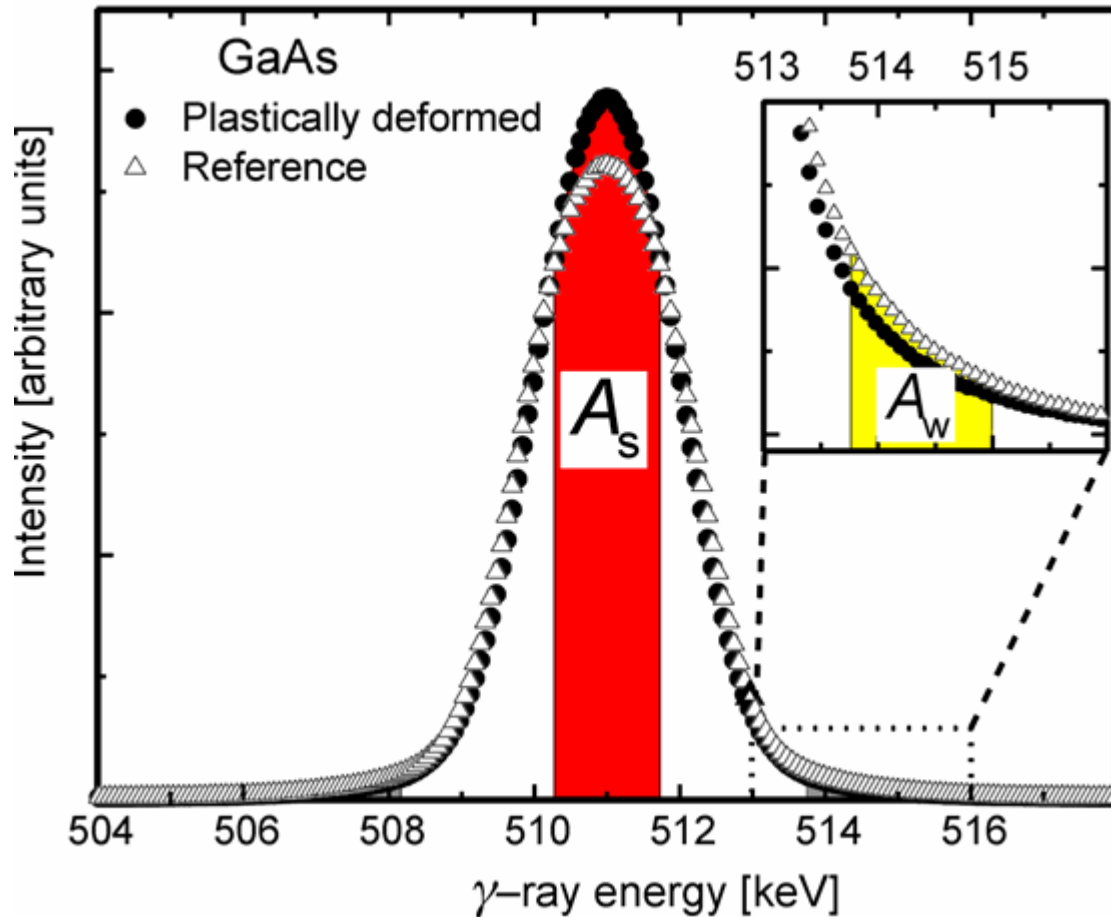
- in a metal: charge of a vacancy is effectively screened by free electrons
- they are not available in semiconductors
- thus, long-range Coulomb potential added
- positrons may be attracted or repelled
- trapping coefficient μ is function of charge state

Measurement of Doppler Broadening



- electron momentum in propagation direction of 511 keV γ -ray leads to Doppler broadening of annihilation line
- can be detected by conventional energy-dispersive Ge detectors and standard electronics

Line Shape Parameters



S parameter:

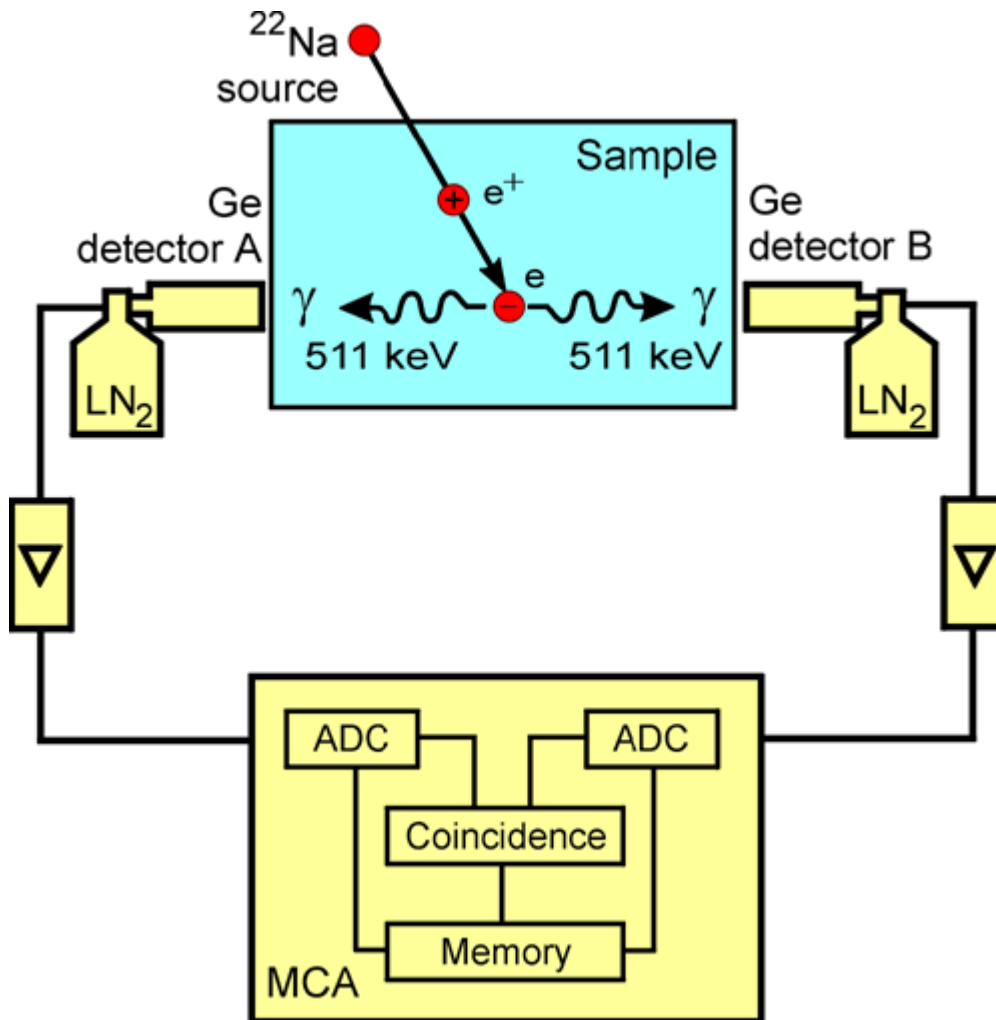
$$S = A_S/A_0$$

W parameter:

$$W = A_W/A_0$$

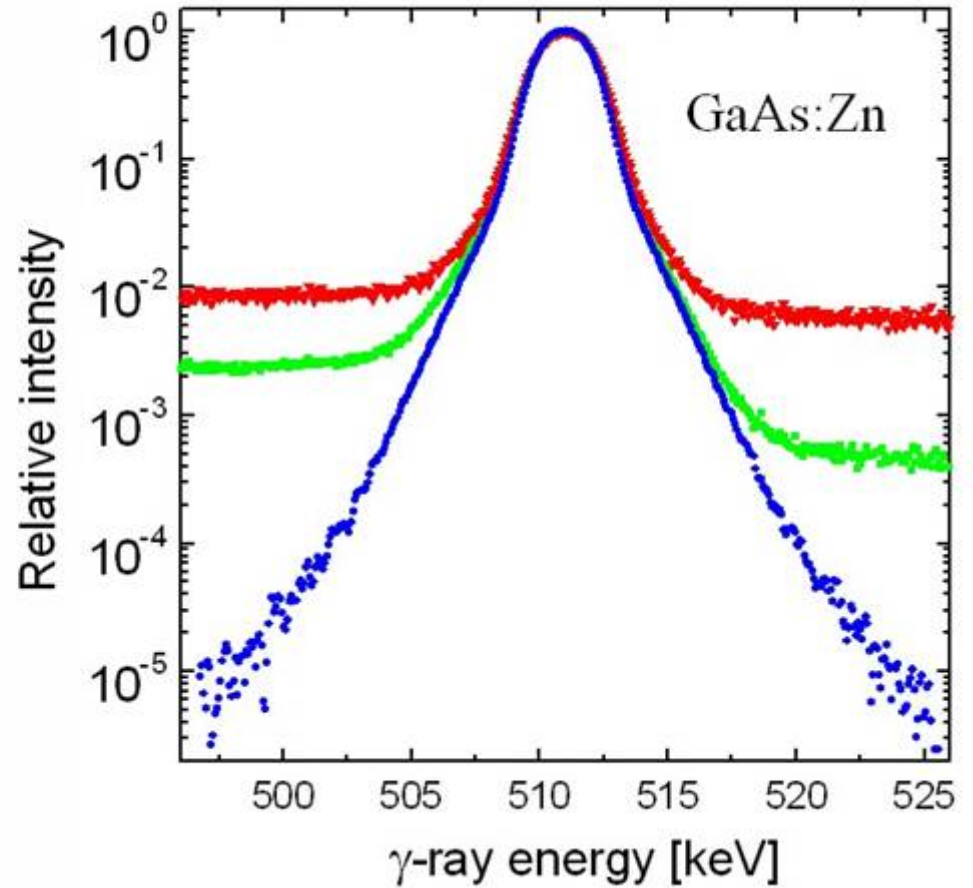
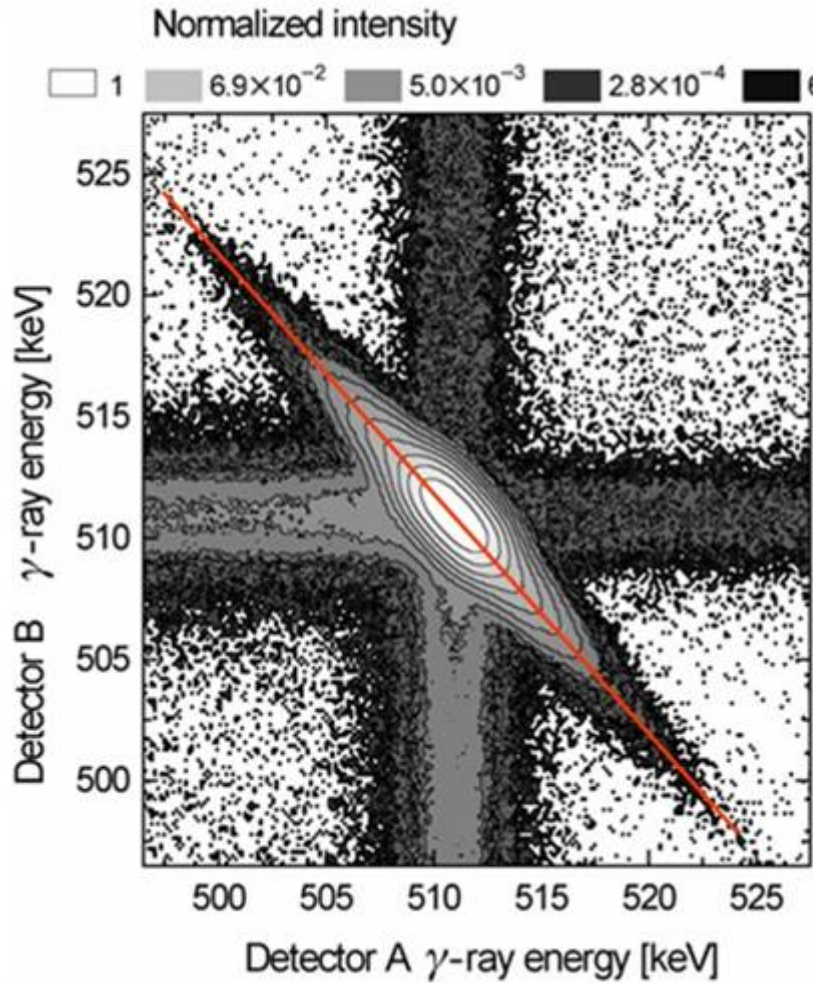
W parameter mainly determined by annihilations of core electrons (chemical information)

Doppler Coincidence Spectroscopy



- coincident detection of second annihilation γ reduces background
- use of a second Ge detector improves energy resolution of system

Doppler Coincidence Spectra

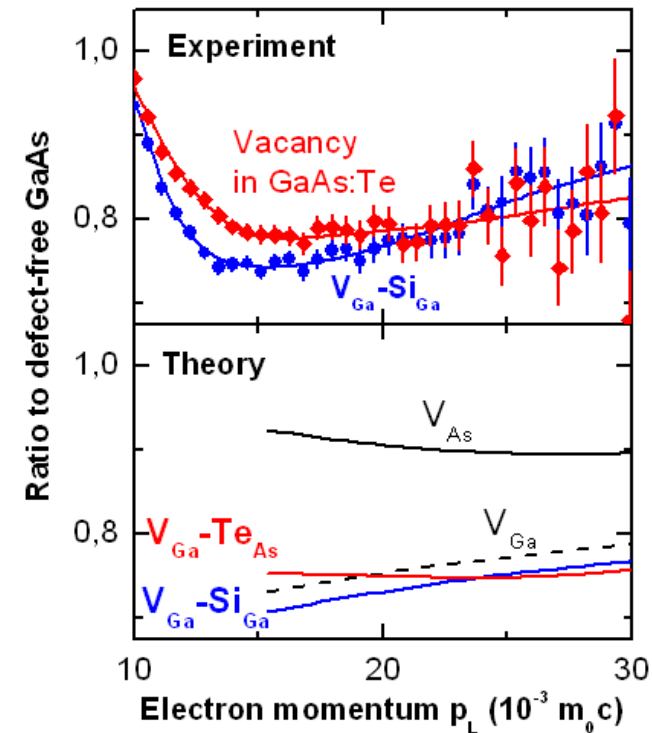
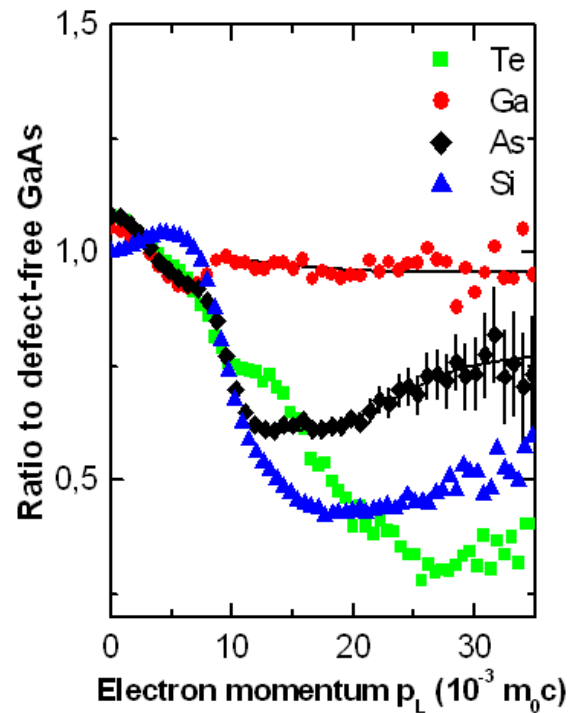
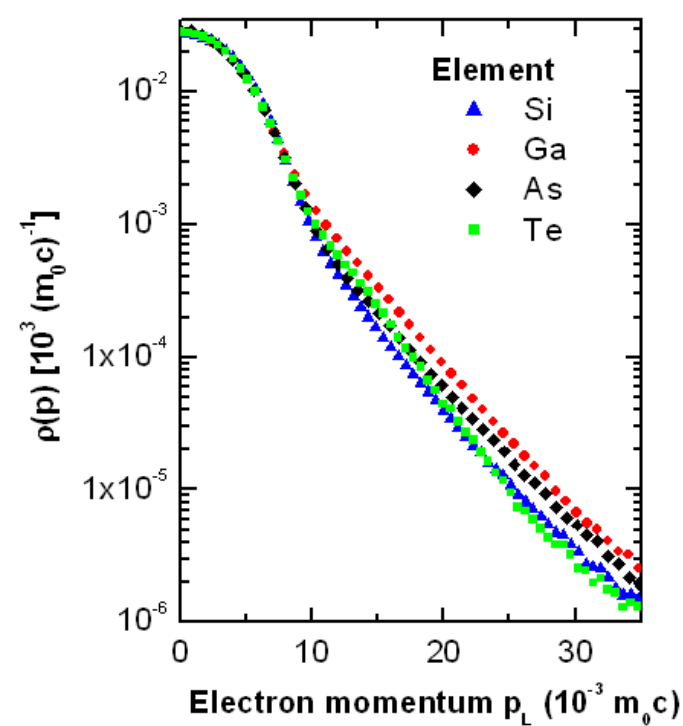


$$E_1 + E_2 = 2 m_0 c^2 = 1022 \text{ keV}$$



Doppler-Coincidence-Spectroscopy in GaAs

- Chemical sensitivity due to electrons at high momentum (core electrons)
- a single impurity atom aside a vacancy is detectable
- examples: $V_{Ga}-Te_{As}$ in GaAs:Te



J. Gebauer et al., Phys. Rev. B **60** (1999) 1464

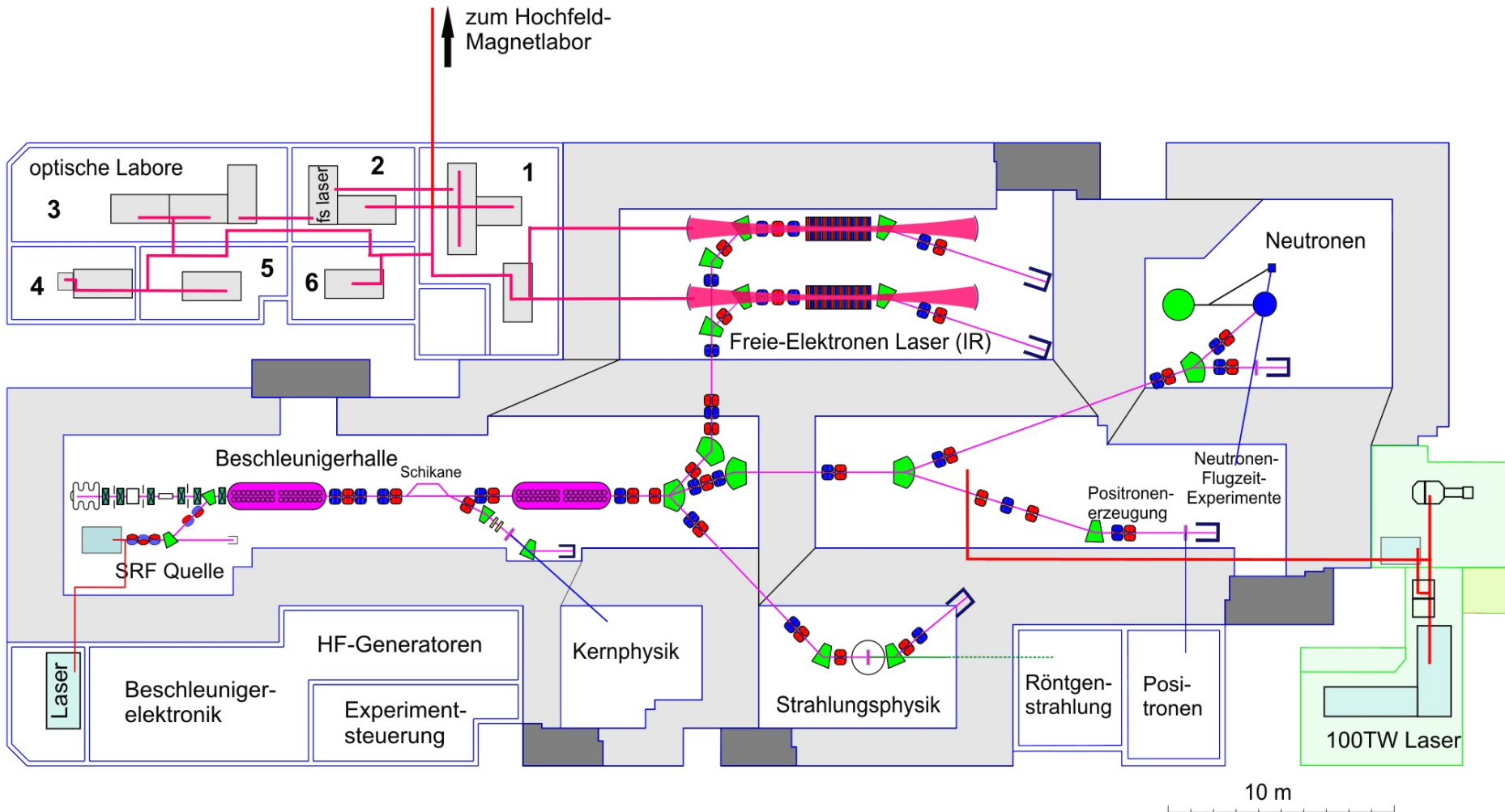


EPOS = ELBE Positron Source

- ELBE -> electron LINAC (40 MeV and up to 40 kW) in Research Center Dresden-Rossendorf
- EPOS will be the combination of a positron lifetime spectrometer, Doppler coincidence, and AMOC
- User-dedicated facility
- main features:
 - ultra high-intensity bunched positron beam ($E_+ = 0.5...30$ keV)
 - good time resolution by using the unique primary time structure of ELBE
 - very high count rate

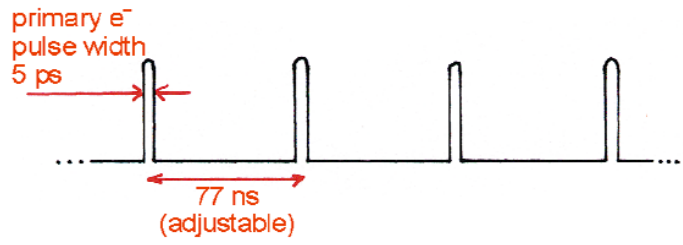
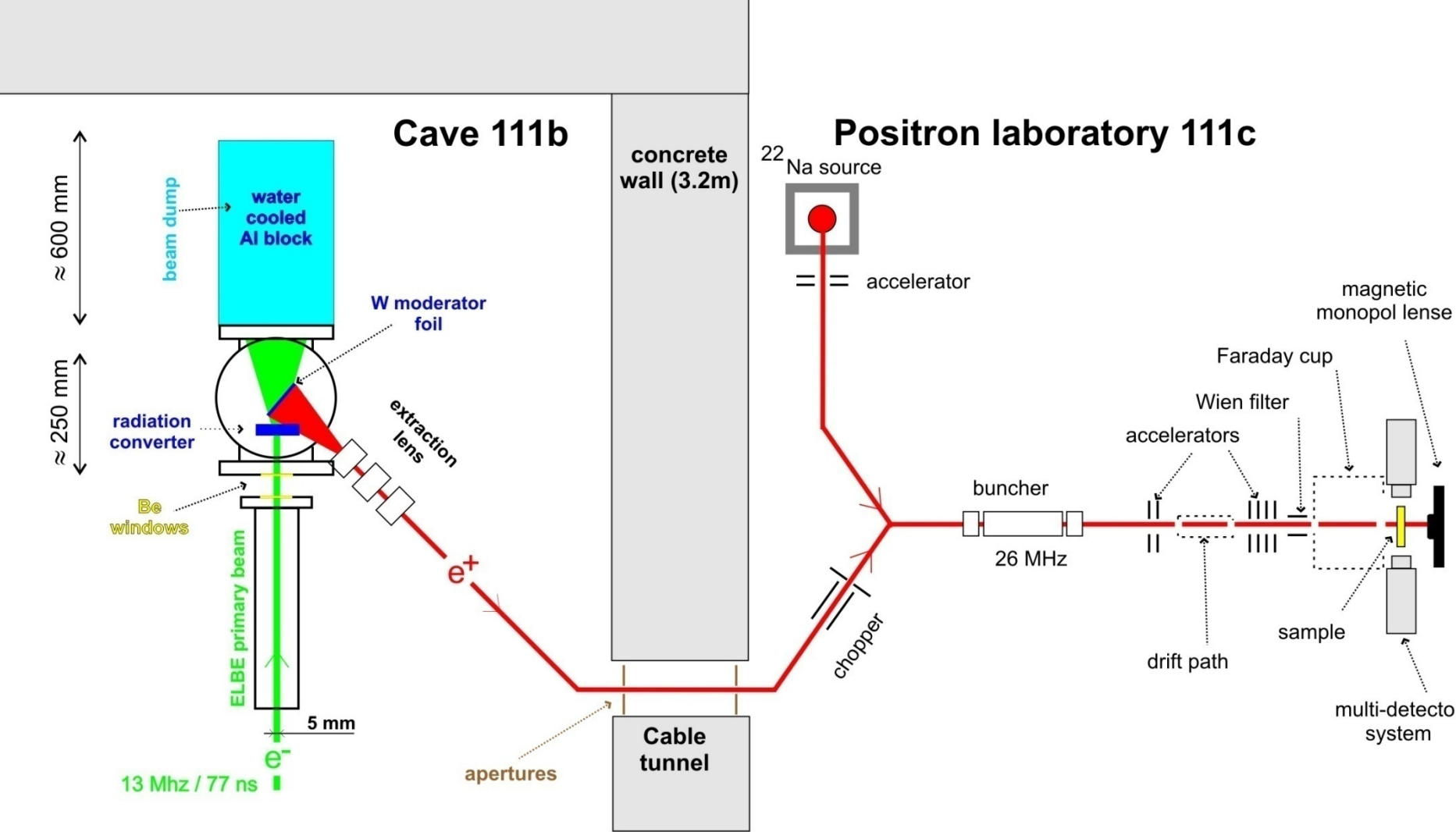


Ground plan of the ELBE hall



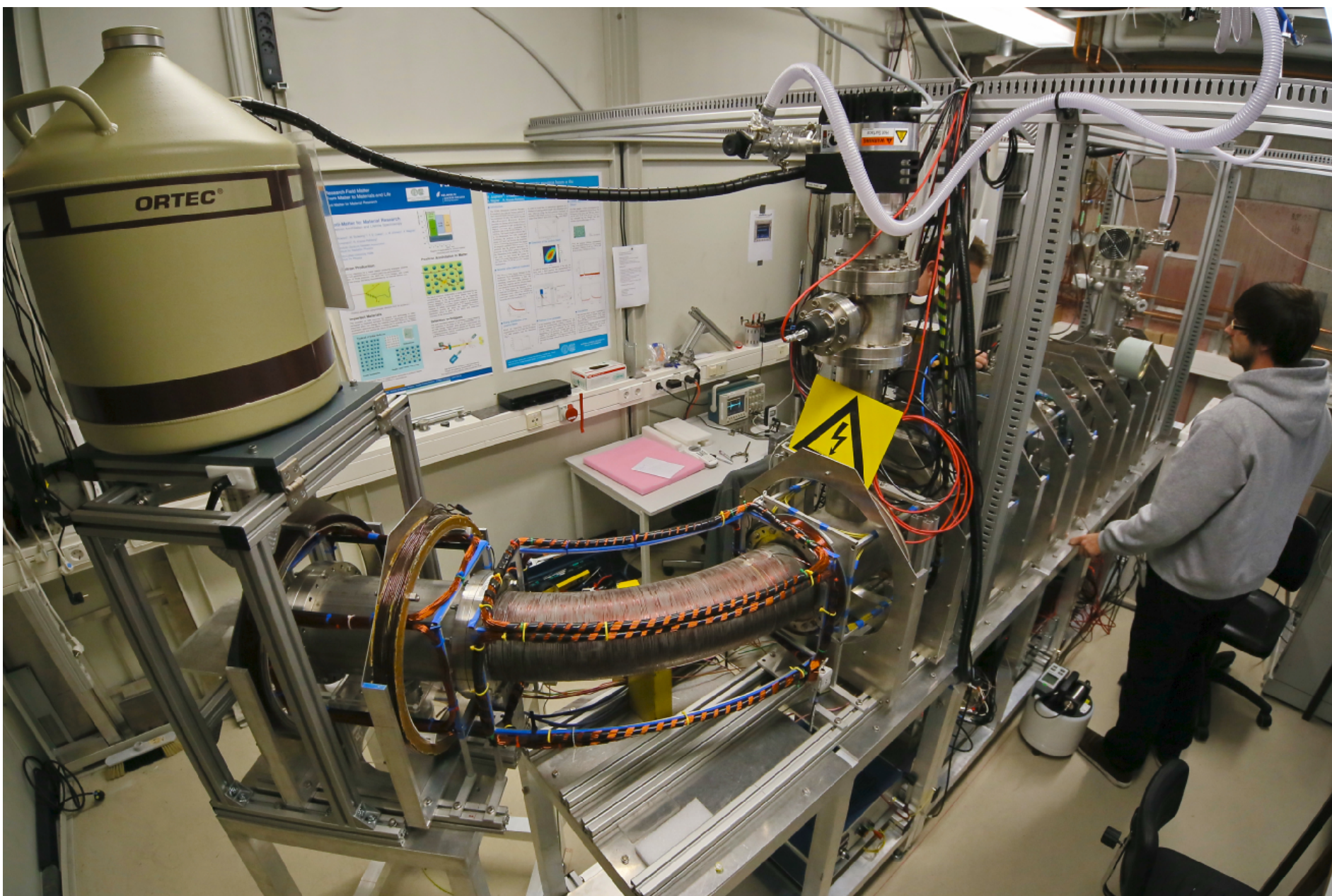
1: Diagnosestation, IR-Imaging und biologische IR Experimente
 2: Femtosekundenlaser, THz-Spektroskopie, IR Pump-Probe Experimente
 3: Zeitaufgelöste Halbleiter-Spektroskopie, THz-Spektroskopie

4: FTIR, biologische IR Experimente
 5: Nahfeld und Pump-Probe IR Experimente
 6: Radiochemie und Summenfrequenz-Erzeugung, photothermische Spektroskopie



MePS scheme



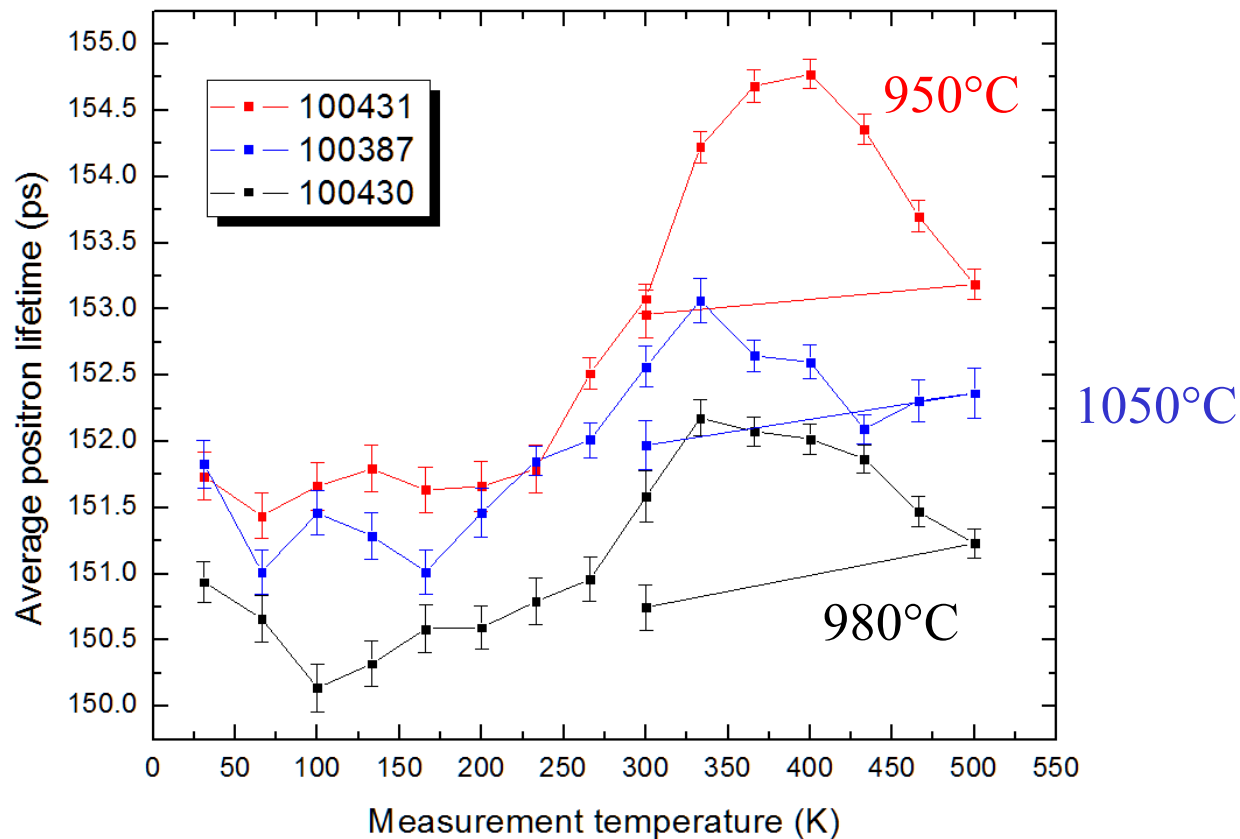


Defect studies of GaN

- as-grown GaN (FCM GmbH) - 2012

Unterschied zwischen den 3 Proben ist die Wachstumstemperatur:

- 100387: 1050°C,
- 100430: 980°C sowie
- 100431: 950°C.



Observation of Native Ga Vacancies in GaN by Positron Annihilation

K. Saarinen,¹ T. Laine,¹ S. Kuisma,¹ J. Nissilä,¹ P. Hautojärvi,¹ L. Dobrzynski,² J. M. Baranowski,³ K. Pakula,³
R. Stepniowski,³ M. Wojdak,³ A. Wyszolek,³ T. Suski,⁴ M. Leszczynski,⁴ I. Grzegory,⁴ and S. Porowski⁴

¹Laboratory of Physics, Helsinki University of Technology, 02150 Espoo, Finland

²Institute of Physics, Warsaw University Branch, Lipowa 41, 15-424 Bialystok, Poland
and Soltan Institute of Nuclear Studies, 05-400 Otwock-Swierk, Poland

³Institute of Experimental Physics, University of Warsaw, 00-681 Warsaw, Poland

⁴UNIPRESS, High Pressure Research Center, Polish Academy of Sciences, 01-142 Warsaw, Poland

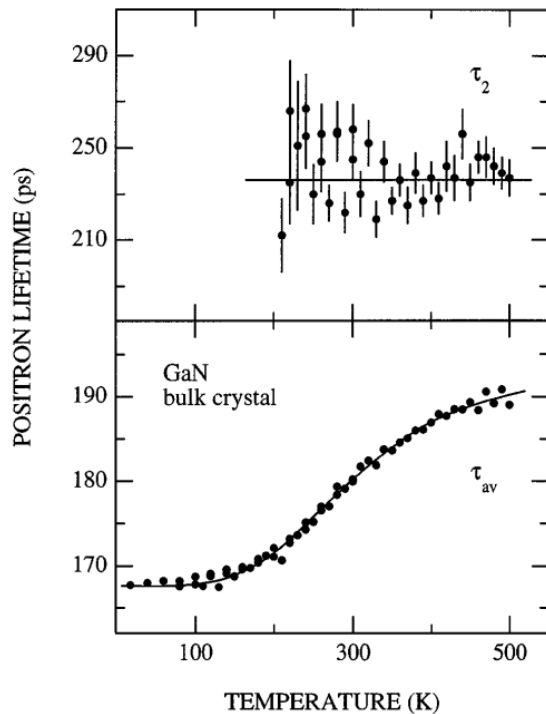


FIG. 1. The average positron lifetime τ_{av} and the lifetime component τ_2 vs measurement temperature GaN bulk crystal. The lifetime component τ_2 could be decomposed only at $T > 200$ K. The solid lines are drawn to guide the eye.

[Ga vacancies] $\approx 10^{18} \text{ cm}^{-3}$

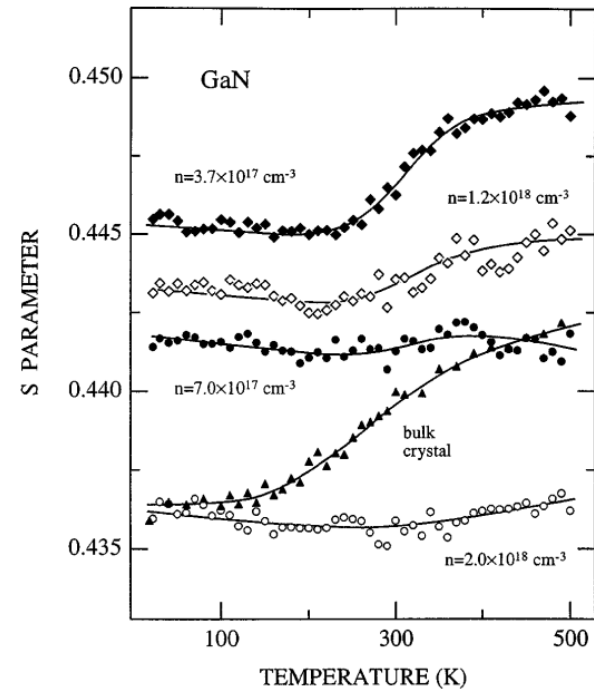


FIG. 2. The low electron-momentum parameter S vs measurement temperature in various GaN samples. The carrier concentrations of the GaN layers at 300 K are indicated in the figure. The solid lines are fits to the temperature dependent positron trapping model (Ref. [14]).



Gallium vacancies and the growth stoichiometry of GaN studied by positron annihilation spectroscopy

K. Saarinen,^{a)} P. Seppälä, J. Oila, P. Hautojärvi, and C. Corbel

Laboratory of Physics, Helsinki University of Technology, P.O. Box 1100, 02015 HUT, Finland

O. Briot and R. L. Aulombard

Université Montpellier II, Groupe d'Etudes des Semiconducteurs, CC074, 34095 Montpellier Cedex 5, France

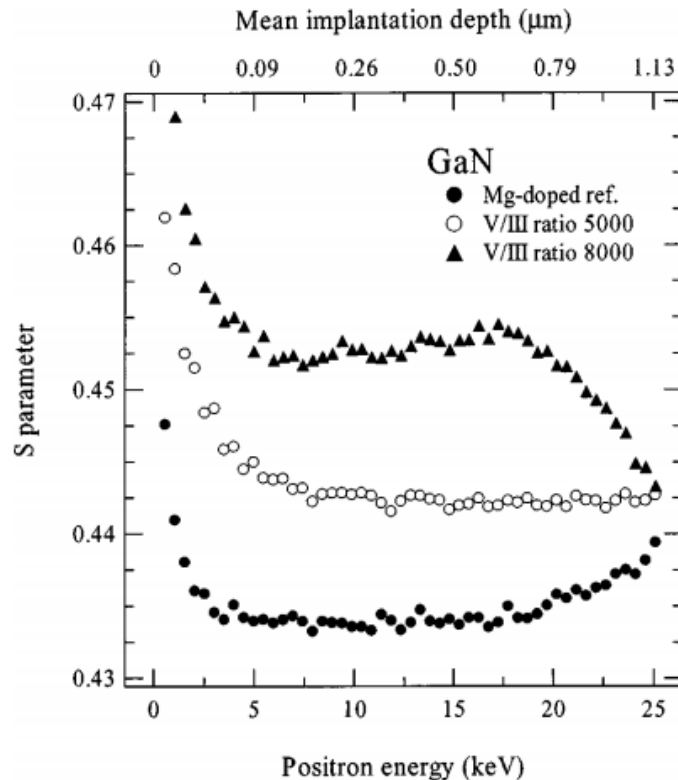


FIG. 1. The low electron-momentum parameter S as a function of the positron implantation energy in three GaN samples. The top axis shows the mean stopping depth corresponding to the positron implantation energy.

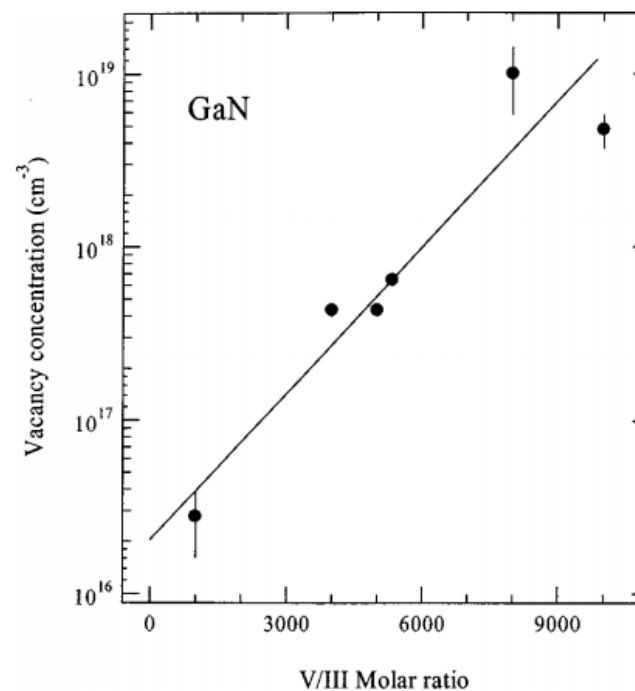


FIG. 3. The concentration of Ga vacancies vs the V/III molar ratio in undoped GaN samples. The straight line is drawn to emphasize the correlation.

The influence of Mg doping on the formation of Ga vacancies and negative ions in GaN bulk crystals

K. Saarinen,^{a)} J. Nissilä, and P. Hautojärvi
Laboratory of Physics, Helsinki University of Technology, FIN-02015 HUT, Finland

J. Likonen
Technical Research Centre of Finland, Chemical Technology, FIN-02044 VTT, Finland

T. Suski, I. Grzegory, B. Lucznik, and S. Porowski
UNIPRESS, High Pressure Research Center, Polish Academy of Sciences, 01-142 Warsaw, Poland

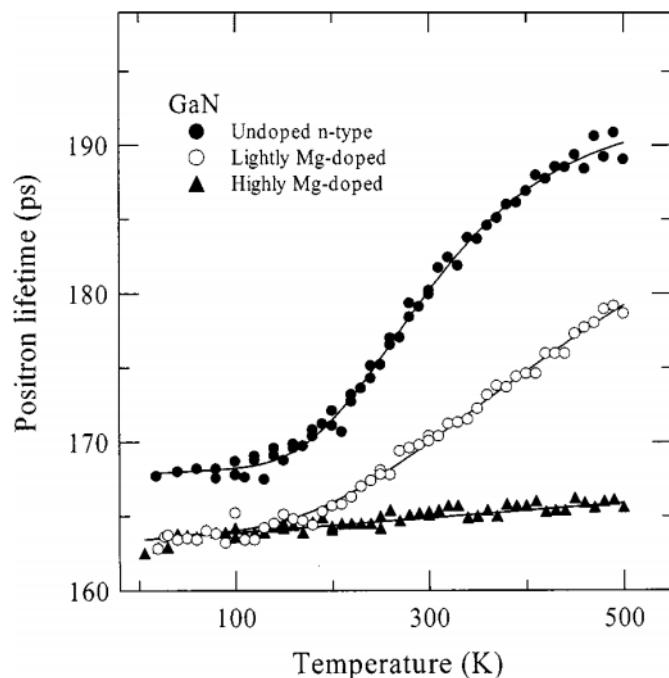


FIG. 2. Average positron lifetime vs measurement temperature in GaN bulk crystals. The solid lines correspond to the analyses with the temperature-dependent positron trapping model, where concentrations of Ga vacancies and negative ions (Table I) are determined as fitting parameters.

In conclusion, the positron experiments show the presence of Ga vacancies and negative ions in GaN crystals. The concentration of Ga vacancies decreases with increasing Mg doping, in good agreement with the trends expected for the V_{Ga} formation energy as a function of the Fermi level. The concentration of negative ions increases with Mg doping and correlates with the Mg concentration determined by SIMS. We thus associate the negative ions with Mg_{Ga}^- . The negative charge of Mg suggests that the loss of n -type conductivity in the Mg doping of GaN crystals is mainly due to compensation of O_{N}^+ donors by Mg_{Ga}^- acceptors.

Ga vacancies in electron irradiated GaN: introduction, stability and temperature dependence of positron trapping

K. Saarinen^{a,*}, T. Suski^b, I. Grzegory^b, D.C. Look^c

^aLaboratory of Physics, Helsinki University of Technology, P.O. Box 1100, 02150 HUT, Finland

^bUNIPRESS, High Pressure Research Center, Polish Academy of Sciences, 01-142 Warsaw, Poland

^cSemiconductor Research Center, Wright State University, Dayton, OH, USA

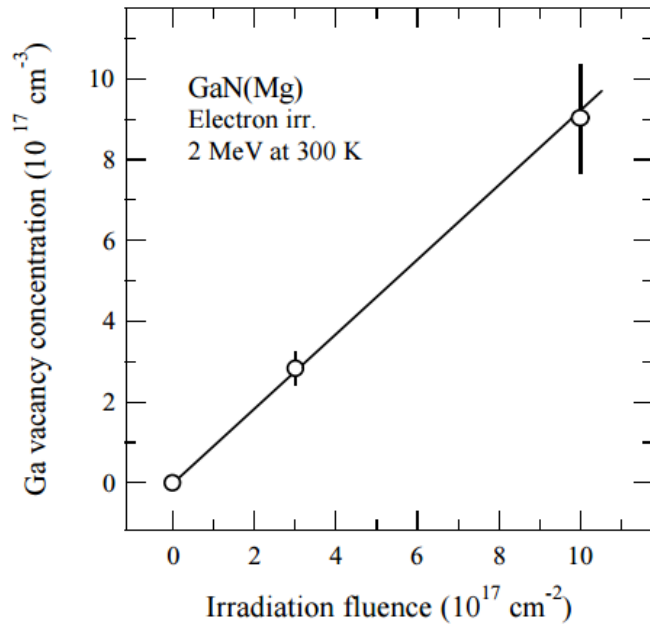


Fig. 3. The concentration of Ga vacancies as a function of 2 MeV electron irradiation fluence at 300 K. The solid line corresponds to the introduction rate of $\Sigma_V = 1 \text{ cm}^{-1}$ [3].

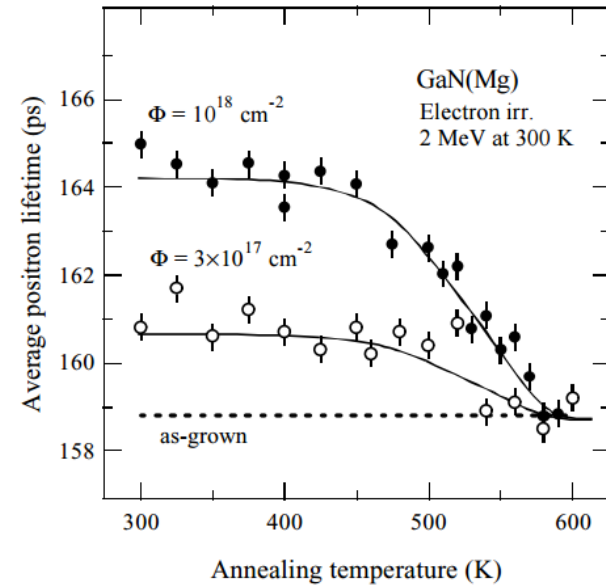


Fig. 1. Average positron lifetime as a function of annealing temperature T_{ann} in two GaN samples irradiated to fluences Φ . The measurement temperature was $T_{\text{meas}} = 300 \text{ K}$. The dashed line shows the level of the average positron lifetime in as-grown samples before irradiation [3].

Ga vacancies as dominant intrinsic acceptors in GaN grown by hydride vapor phase epitaxy

J. Oila, J. Kivioja, V. Ranki, and K. Saarinen^{a)}

Laboratory of Physics, Helsinki University of Technology, P.O. Box 1100, FIN-02015 HUT, Finland

D. C. Look

Semiconductor Research Center, Wright State University, Dayton, Ohio

R. J. Molnar

Massachusetts Institute of Technology, Lincoln Laboratory, Lexington, Massachusetts 02420-9108

S. S. Park, S. K. Lee, and J. Y. Han

Samsung Advanced Institute of Technology, P.O. Box 111, Suwon, Korea 440-600

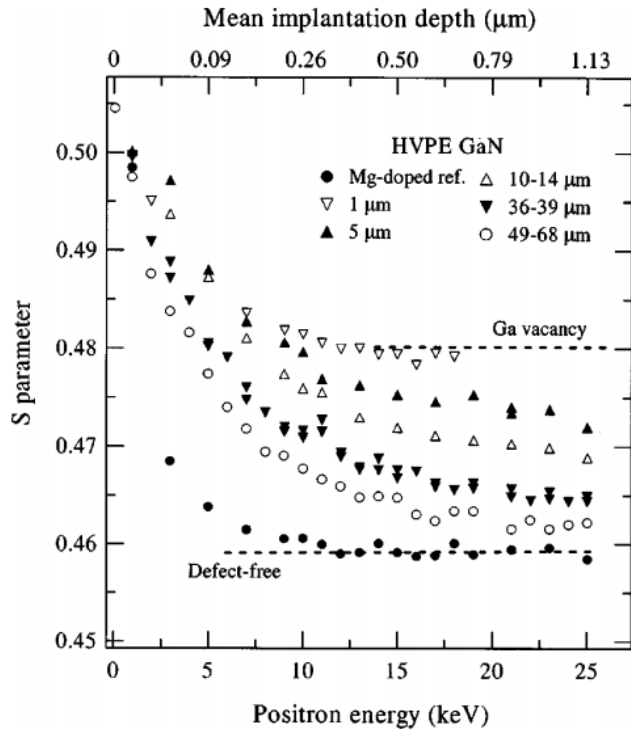


FIG. 2. The low electron-momentum parameter S as a function of the positron implantation energy. The dashed lines show the values of S parameter in defect-free GaN and at the Ga vacancy. The top axis indicates the mean stopping depth corresponding to the positron implantation energy.

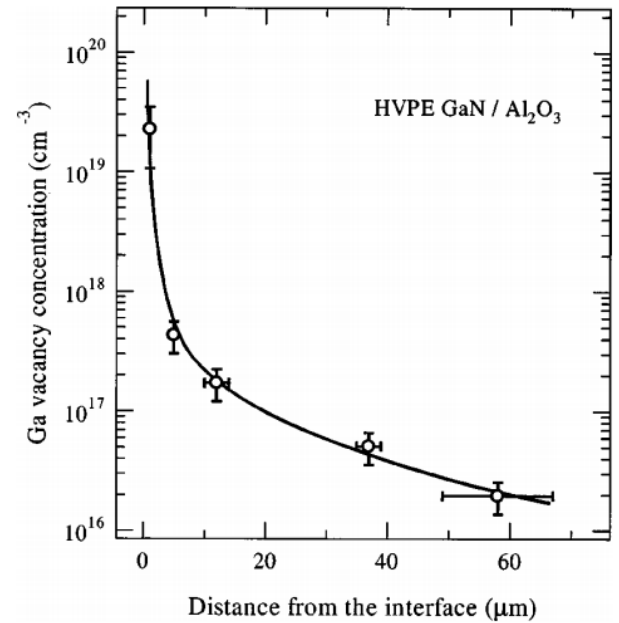


FIG. 3. The concentration of Ga vacancies as a function of the thickness of the GaN layers on sapphire.

In summary, our positron annihilation experiments show that Ga vacancies are the dominant acceptors n -type GaN grown by hydride vapor phase epitaxy on sapphire. The concentration of Ga vacancies decreases from almost 10^{20} cm^{-3} to less than 10^{16} cm^{-3} when the thickness of the GaN layers increases from 1 to more than 100 μm . Furthermore, the Ga vacancy concentration is equal to the total acceptor density determined by temperature-dependent Hall experiments. The depth profile of Ga vacancies is similar to that of O, suggesting that the Ga vacancies formed during the growth are bound to defect complexes with the oxygen impurities.

Direct evidence of impurity decoration of Ga vacancies in GaN from positron annihilation spectroscopy

S. Hautakangas, I. Makkonen, V. Ranki, M. J. Puska, and K. Saarinen*

Laboratory of Physics, Helsinki University of Technology, P.O.Box 1100, FIN-02150 Espoo, Finland

X. Xu

ATMI Inc., 7 Commerce Drive, Danbury, Connecticut 06810, USA

D. C. Look

Semiconductor Research Center, Wright State University, Dayton, Ohio 45435, USA

(Received 27 February 2006; published 3 May 2006)

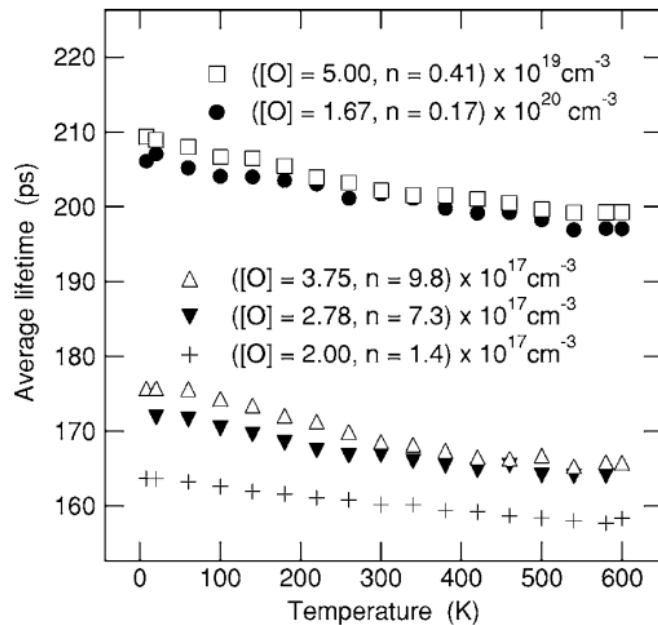


FIG. 1. The average positron lifetime as a function of measuring temperature. The first number in the parentheses stands for O concentration and the second one indicates the free carrier concentration.

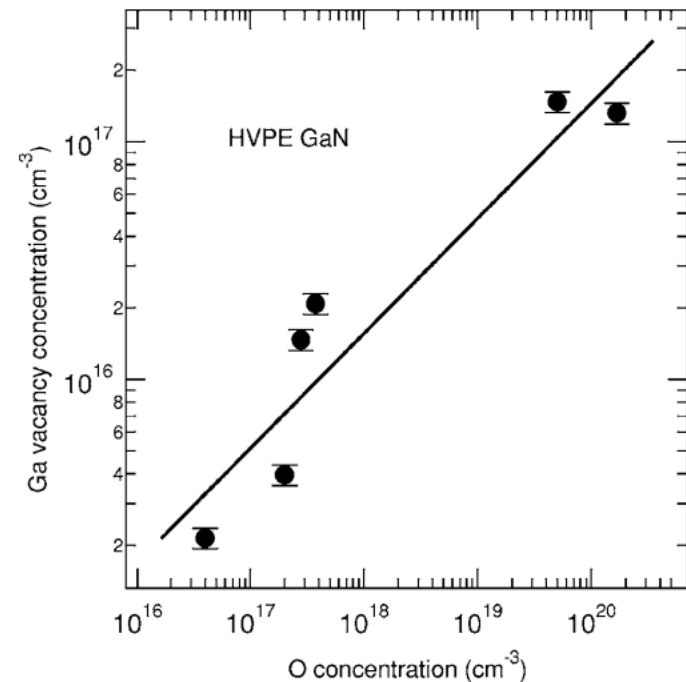


FIG. 2. Gallium vacancy concentration as a function of doping. The solid line is a guide to the eye. The results in the sample with the lowest O concentration have been taken from Ref. 18.

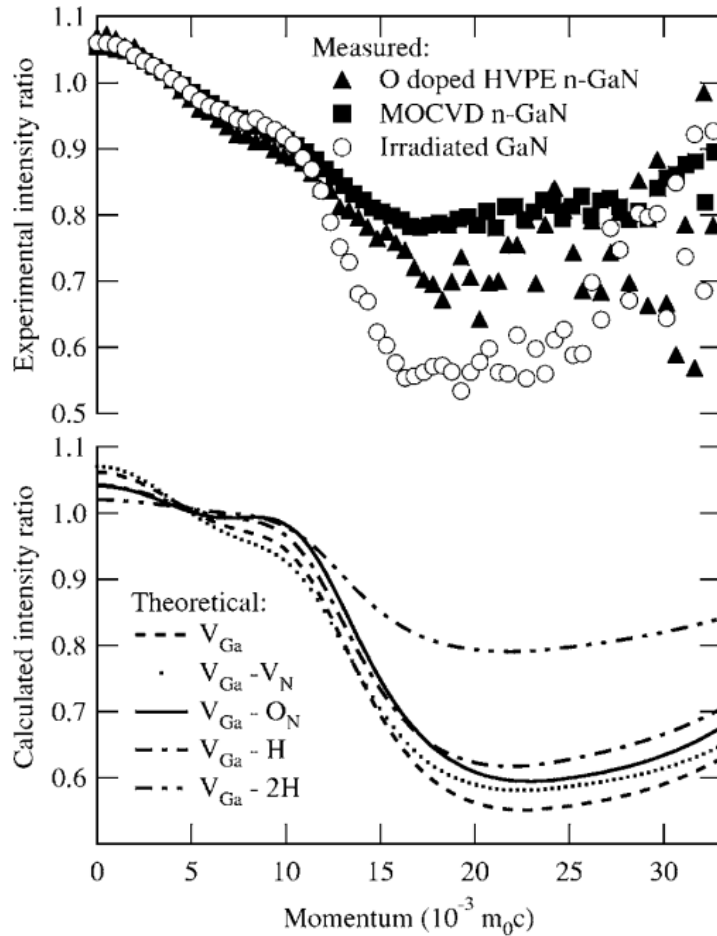


FIG. 4. Measured and calculated momentum distribution curves for different types of samples and defects, respectively. All these curves are shown as ratios to the data obtained in the GaN lattice.

We identify the isolated V_{Ga} in undoped electron irradiated GaN, and show that in O-doped HVPE GaN the Ga vacancy is complexed with the O atom forming $V_{Ga}-O_N$ -pairs. In MOCVD material our data show that the Ga vacancy is likely to be decorated by both oxygen and hydrogen.

Vacancy-type defects in Er-doped GaN studied by a monoenergetic positron beam

A. Uedono,^{1,a)} C. Shaoqiang,¹ S. Jongwon,¹ K. Ito,¹ H. Nakamori,¹ N. Honda,¹
 S. Tomita,¹ K. Akimoto,¹ H. Kudo,¹ and S. Ishibashi²

¹*Institute of Applied Physics, University of Tsukuba, Tsukuba, Ibaraki, 305-8573, Japan*

²*Research Institute for Computational Sciences, National Institute of Advanced Industrial Science and Technology, Tsukuba, Ibaraki, 305-8568, Japan*

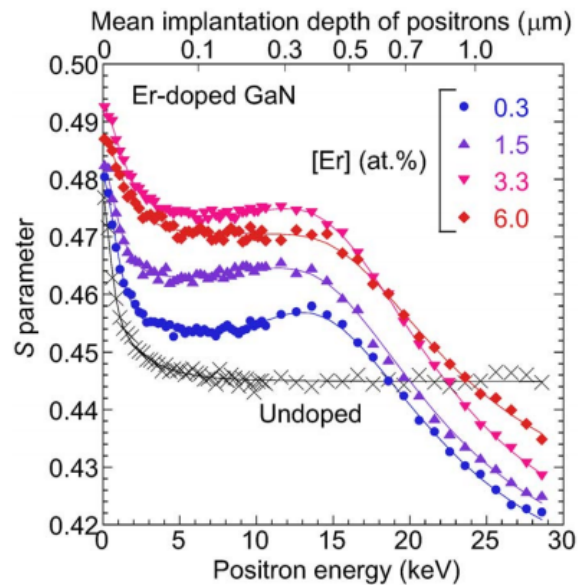


FIG. 1. (Color online) S as a function of incident positron energy E for Er-doped GaN with $[Er]=0.3-6.0$ at. %. The result for undoped GaN is also shown. The S values at $E \leq 14$ keV correspond to the annihilation of positrons in the GaN layers. The solid curves are fits to the experimental data. The derived depth distributions of S are shown in Fig. 3.

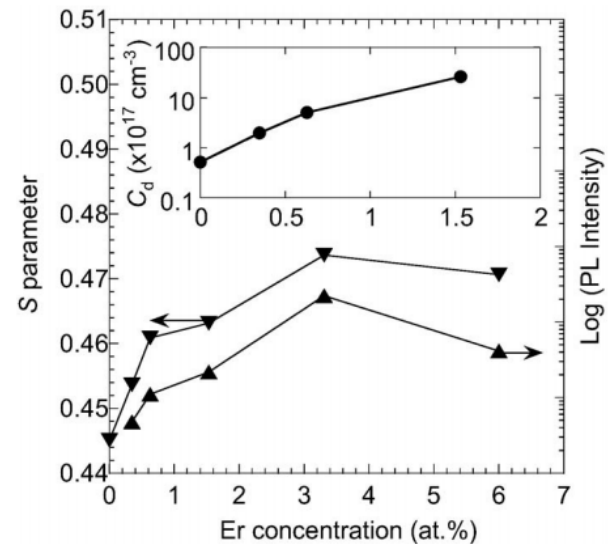


FIG. 2. S values corresponding to the annihilation of positrons in Er-doped GaN and the integrated intensities of a 551 nm PL line as a function of the Er concentration, where the PL intensity is shown in a logarithmic scale. The inset shows the concentration of Ga vacancies (V_{Ga}) derived from the positron trapping model.



Microstructural evolution in H ion induced splitting of freestanding GaN

O. Moutanabbir,^{1,a)} R. Scholz,¹ S. Senz,¹ U. Gösele,¹ M. Chicoine,² F. Schiettekatte,²
F. Süßkraut,³ and R. Krause-Rehberg³

¹Max Planck Institute of Microstructure Physics, Weinberg 2, D 06120 Halle, Germany

²Département de Physique, Université de Montréal, Succursale Centre Ville, Montréal, Québec, H3T 1J4, Canada

³Department of Physics, Martin-Luther-University Halle-Wittenberg, Friedemann-Bach-Platz 6, D 06108 Halle, Germany

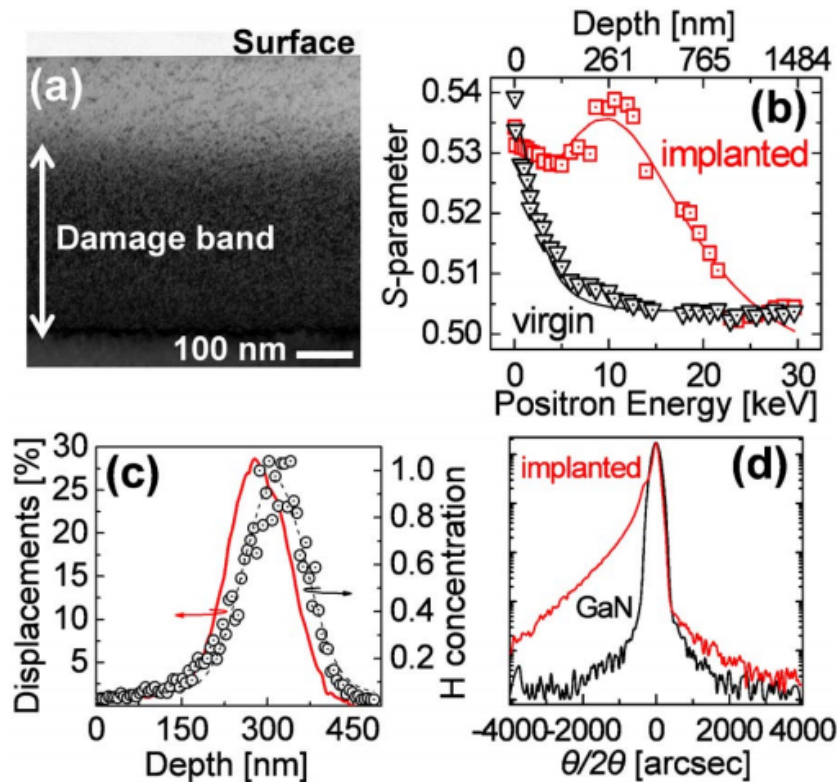


FIG. 1. (Color online) (a) XTEM image of damage induced in GaN by H ion implantation at 50 keV with a fluence of 2.6×10^{17} atom/cm². (b) S parameter depth profile measured before (triangles) and after (squares) H implantation. (c) H concentration/10²² cm⁻³ depth profile (circles) and implantation damage profile (line) as deduced from ERD and ion channeling, respectively. (d) X-ray $\theta/2\theta$ scans of (0002) GaN before and after H implantation.

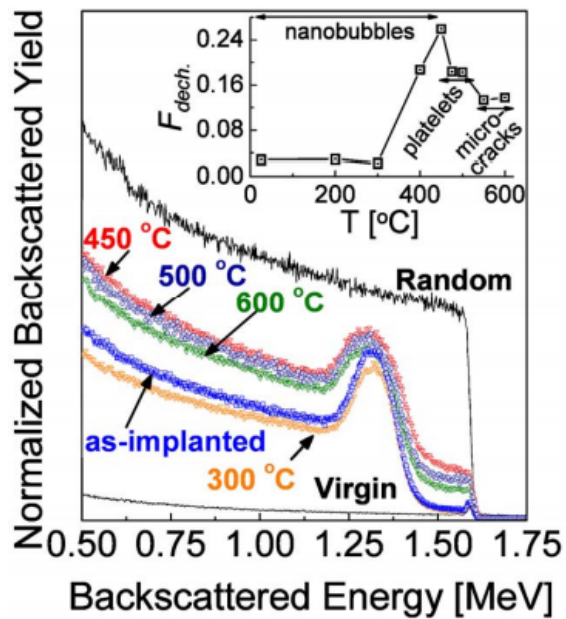


FIG. 2. (Color online) RBS/C yields as a function of annealing temperature for GaN substrates implanted with H at 2.6×10^{17} atom/cm². Inset: Evolution of dechanneling factor F_{dech} , as a function of temperature. The corresponding morphologies, as determined by XTEM, are also indicated.

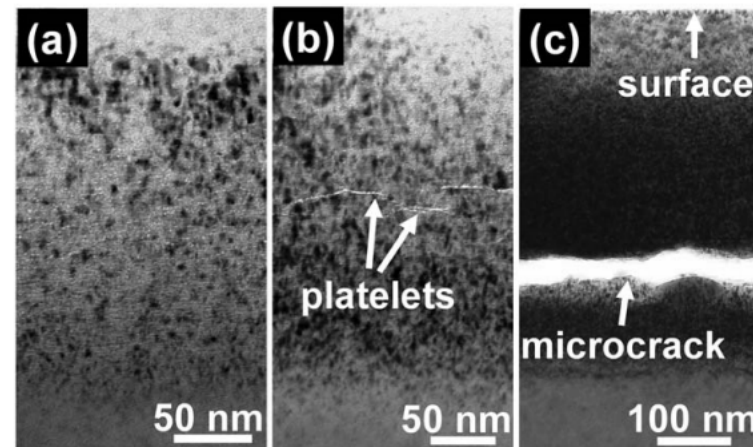


FIG. 3. XTEM micrographs of H-implanted GaN annealed at different temperatures: 450 °C (a), 500 °C (b), and 600 °C (c).

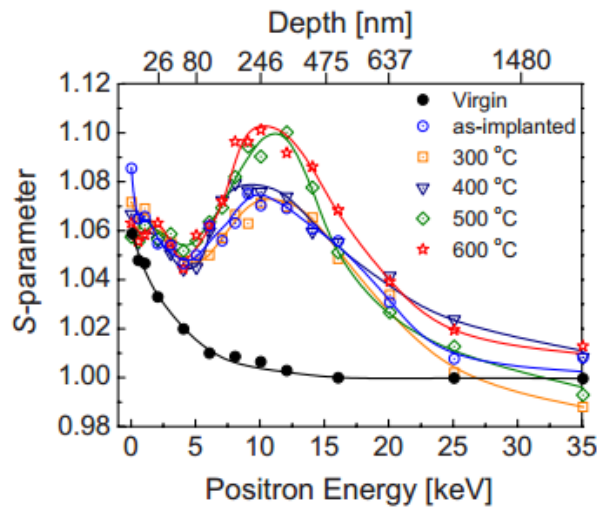


FIG. 3. (Color online) Thermoevolution of the normalized S parameter of H-implanted GaN samples as a function of incident positron energy. For comparison, the spectrum recorded from bulk GaN is also shown.

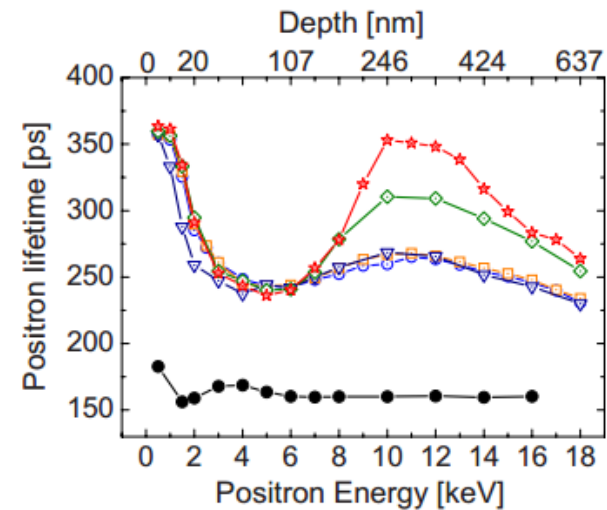


FIG. 4. (Color online) The evolution of the average positron lifetime as a function of the positron energy for the virgin, as-implanted, and annealed GaN samples. The symbols are the same as in Fig. 3.

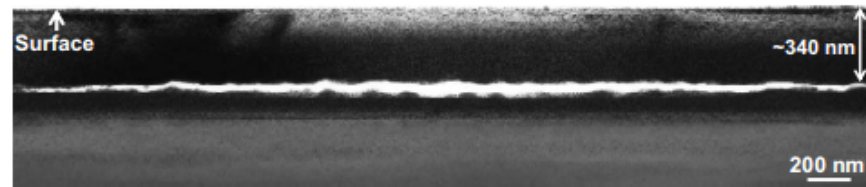


FIG. 2. XTEM image of H-implanted GaN substrate implanted under the conditions described in Fig. 1 and annealed at 600 °C for 5 min.

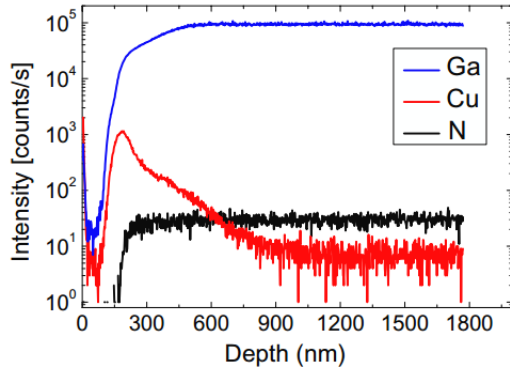


Figure 1. SIMS depth profiles of GaN sample after Cu diffusion induced by annealing for 96 h at 873 K. Note that surface peaks are artifacts of the SIMS measurements.

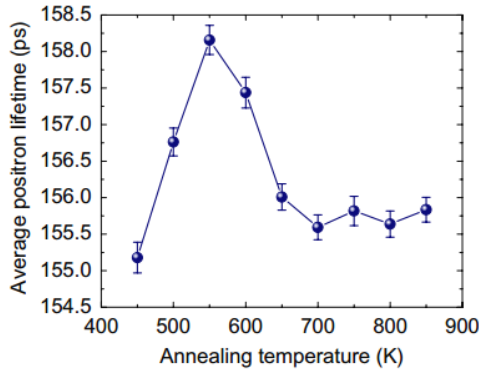


Figure 4. Average positron lifetime of Cu-diffused fs-GaN samples after the isochronal annealing. The spectra were measured at a sample temperature of 333 K.

Cu diffusion-induced vacancy-like defects in freestanding GaN

M Elsayed^{1,6}, R Krause-Rehberg¹, O Moutanabbir^{2,6},
W Anwand³, S Richter⁴ and C Hagedorn⁵

¹ Martin-Luther-University Halle-Wittenberg, von-Danckelmann-Platz 3, Halle (Saale) 06120, Germany

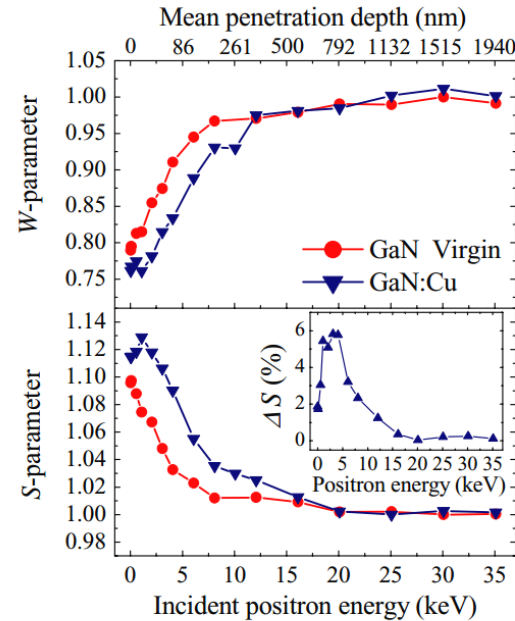


Figure 6. Normalized Doppler broadening parameters as a function of the incident positron energy measured for the virgin and Cu-diffused GaN samples annealed up to 550 K. The low momentum parameter S is shown in the lower panel and W in the upper panel. The positron mean penetration depth is shown in the top axis. The inset of the lower panel displays the difference in S



Conclusions

- Positrons are a unique tool
 - for characterization of vacancy-type defects in crystalline solids
 - for embedded nano-particles (e.g. small precipitates)
 - for porosimetry
- New facilities become available for user-dedicated operation having
 - better time resolution and spectra quality
 - much higher intensity
 - microscope @ FRM-II: lateral resolution 1 μm

This presentation can be found as pdf-file on our Website:
<http://positron.physik.uni-halle.de>

reinhard.krause-rehberg@physik.uni-halle.de



Thank you for your attention!

positron.physik.uni-halle.de

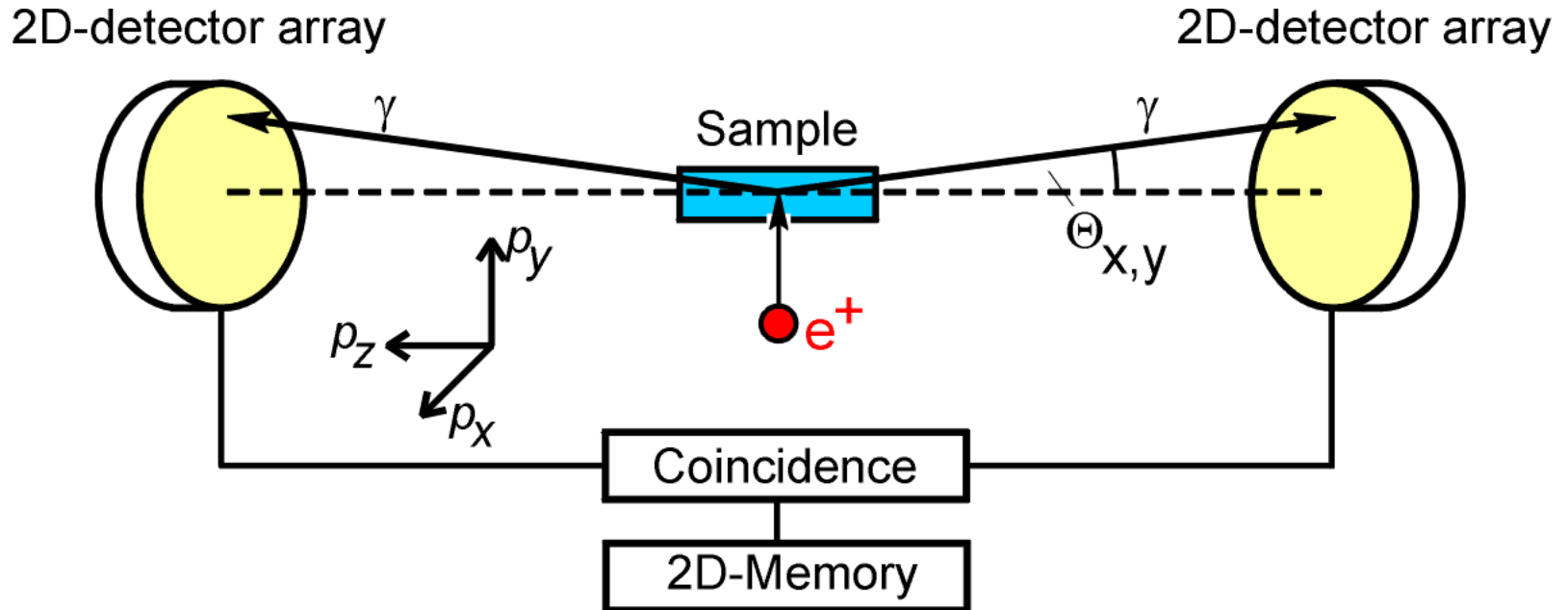
EPOS - Applications

Variety of applications in all field of materials science:

- defect-depth profiles due to surface modifications and ion implantation
- tribology (mechanical damage of surfaces)
- polymer physics (pores; interdiffusion; ...)
- low-k materials (thin high porous layers)
- defects in semiconductors, ceramics and metals
- epitaxial layers (growth defects, misfit defects at interface, ...)
- fast kinetics (e.g. precipitation processes in Al alloys; defect annealing; diffusion; ...)
- radiation resistance (e.g. space materials)
- many more ...



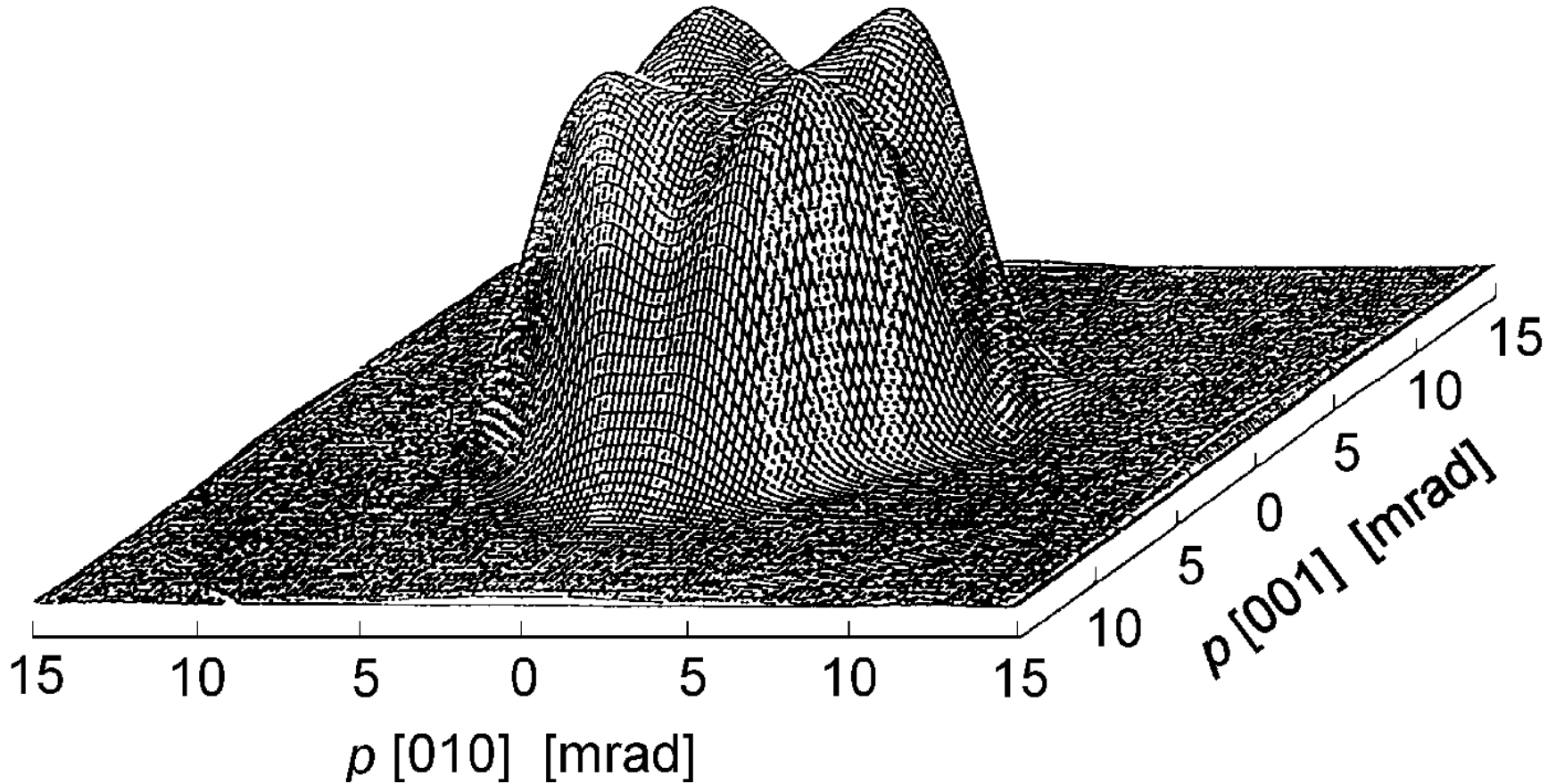
Angular Correlation of Annihilation Radiation - ACAR



Coincidence counting rate N_c :

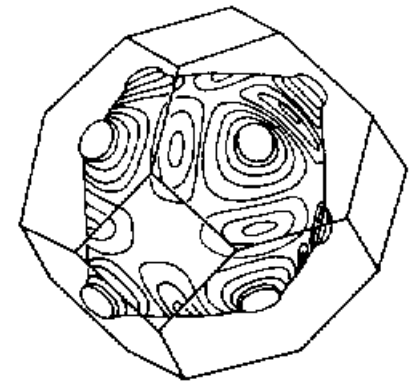
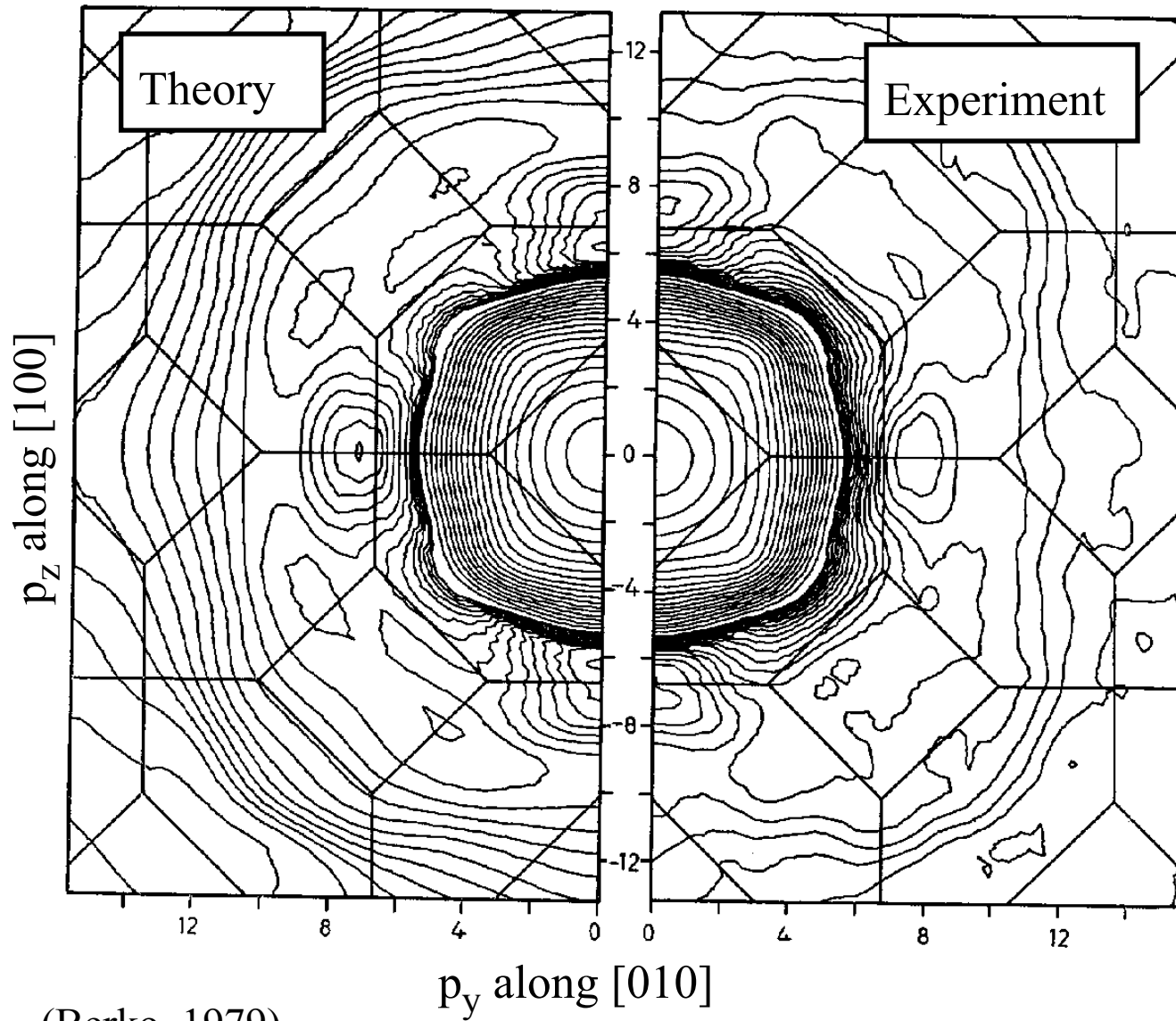
$$N_c(\theta_x, \theta_y) = A_c \int (v_x m_0 c, v_y m_0 c, p_z) dp_z$$

2D-ACAR of defect-free GaAs



(Tanigawa et al., 1995) 3D-Fermi surface can be reconstructed from measurements in several directions of a single crystal

2D-ACAR of Copper

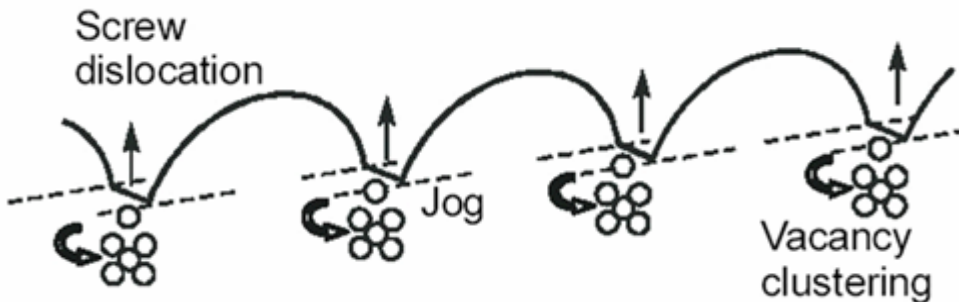
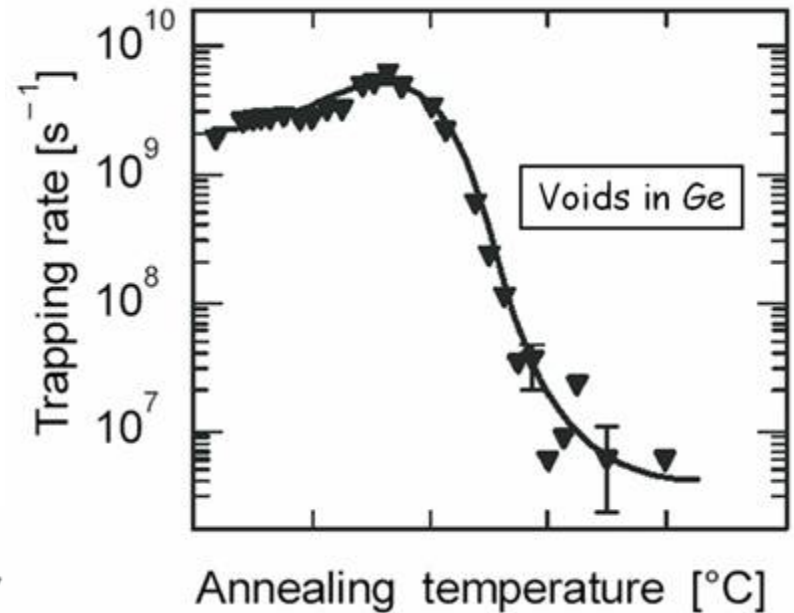


Fermi surface
of copper

(Berko, 1979)

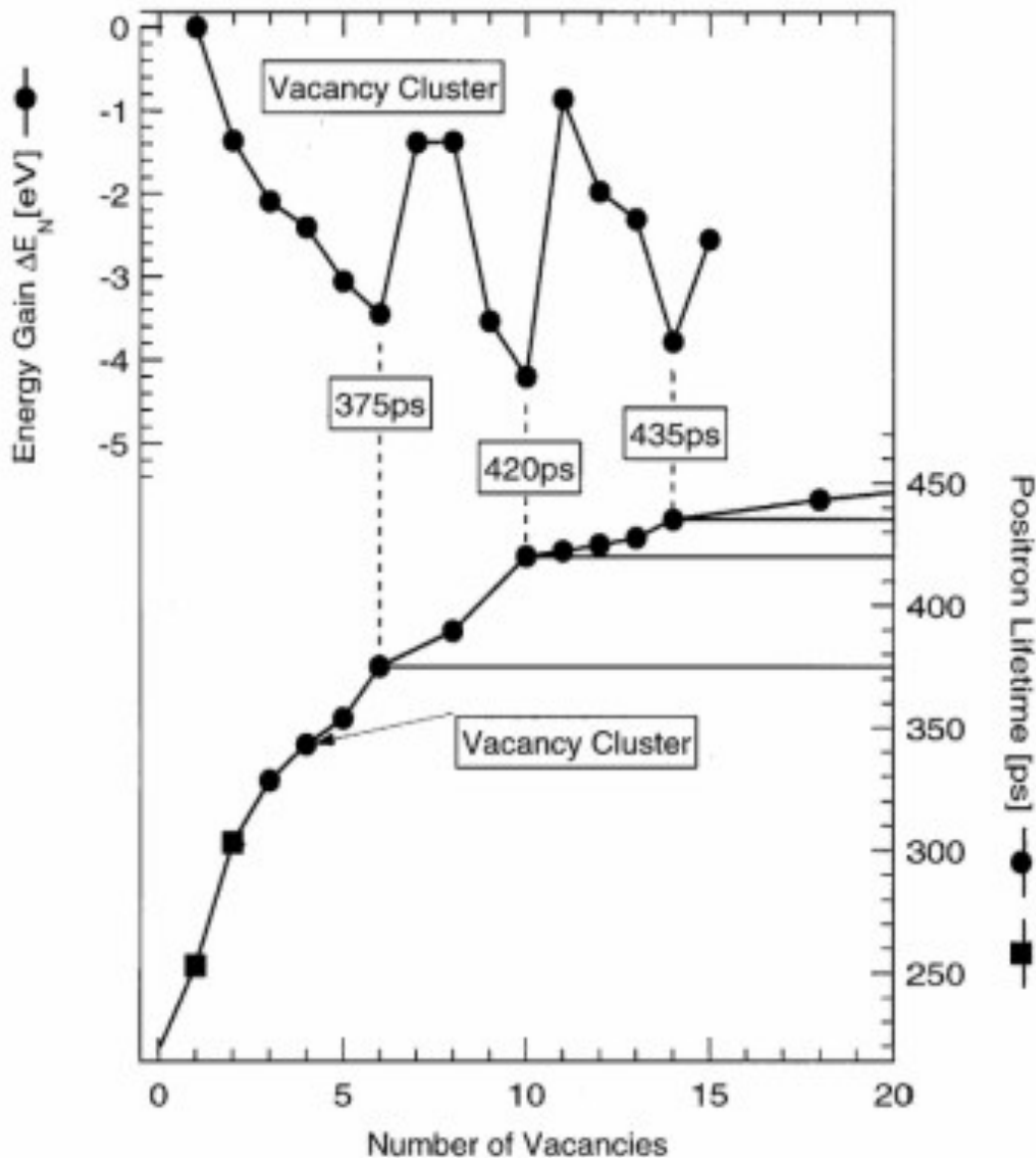
Vacancy clusters in semiconductors

- vacancy clusters were observed after neutron irradiation, ion implantation and plastic deformation
- due to large open volume (low electron density) -> positron lifetime increases distinctly
- example: plastically deformed Ge
- lifetime: $\tau = 525$ ps
- reason for void formation: jog dragging mechanism
- trapping rate of voids disappears during annealing experiment



Krause-Rehberg et al., 1993

Theoretical calculation of vacancy clusters in Si

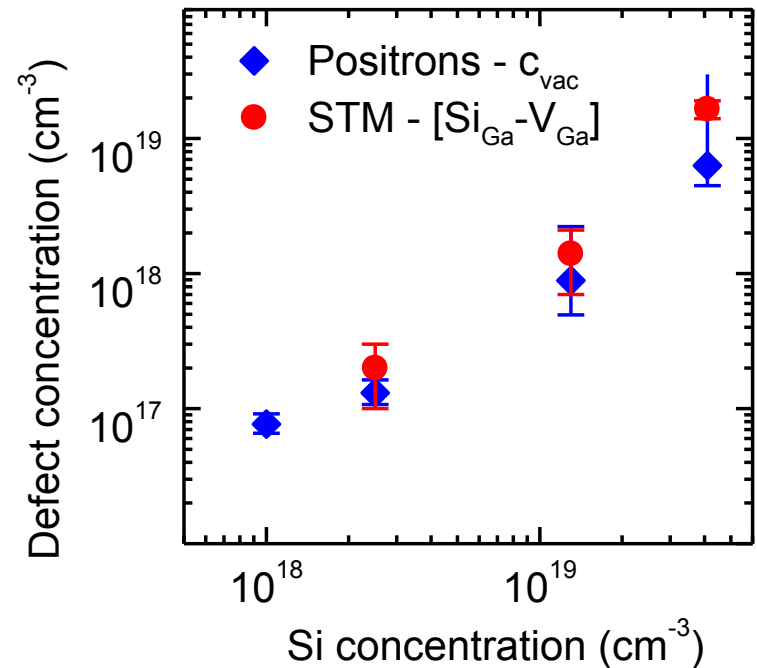
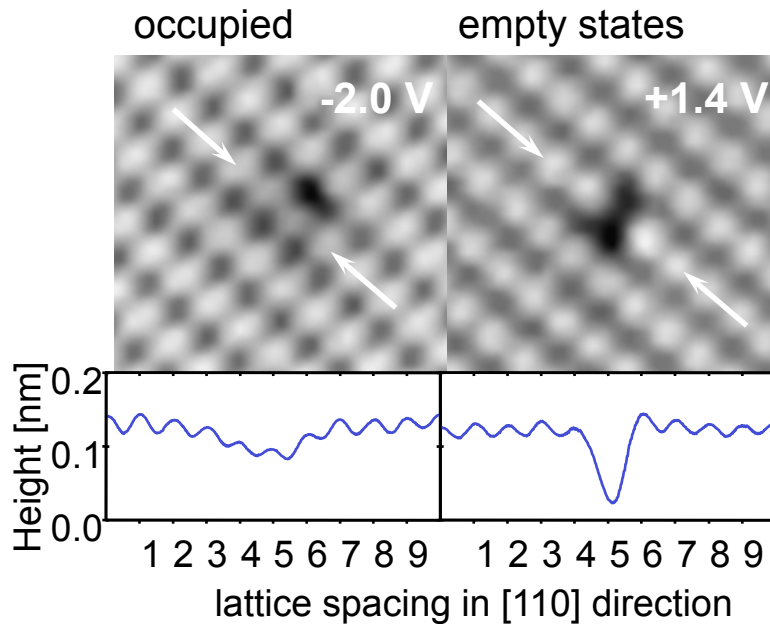


- there are cluster configurations with a large energy gain
- „Magic Numbers“ with 6, 10 und 14 vacancies
- positron lifetime increases distinctly with cluster size
- for $n > 10$ saturation effect, i.e. size cannot be determined

T.E.M. Staab et al.,
Physica B 273-274 (1999) 501-504



Identification of $V_{Ga}-Si_{Ga}$ -Complexes in GaAs:Si



- Scanning tunneling microscopy at GaAs (110)-cleavages planes (by Ph. Ebert, Jülich)
- Defect complex identified as $V_{Ga}-Si_{Ga}$

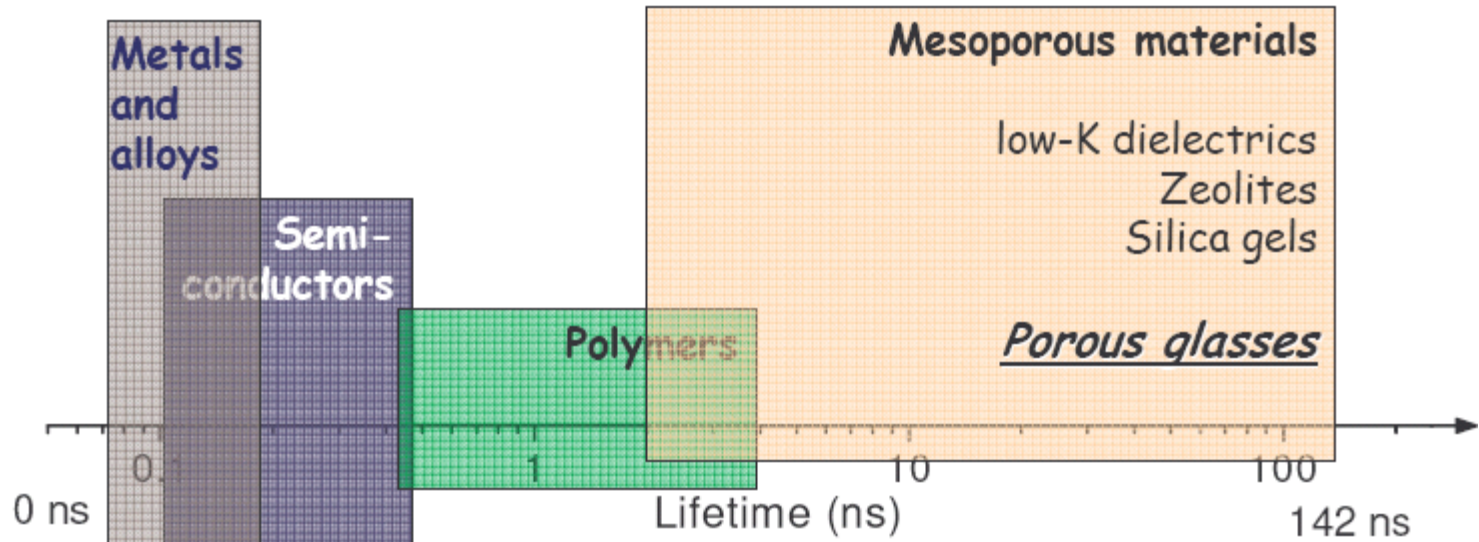
- Quantification \rightarrow Agreement

Mono-Vacancies in GaAs:Si are $V_{Ga}-Si_{Ga}$ -complexes

Gebauer et al., Phys. Rev. Lett. **78** (1997) 3334



Typical Lifetimes



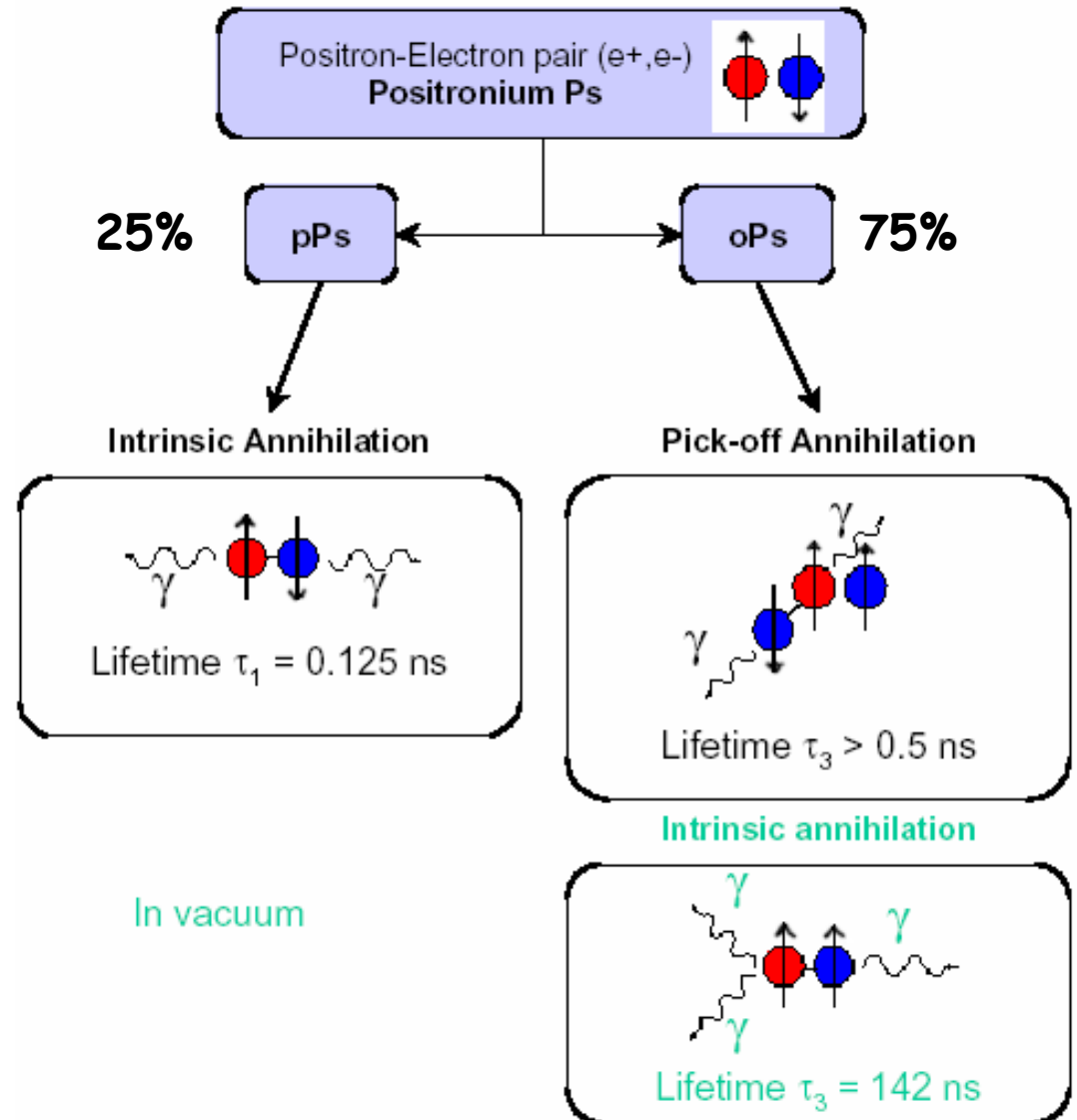
Positron

Positronium



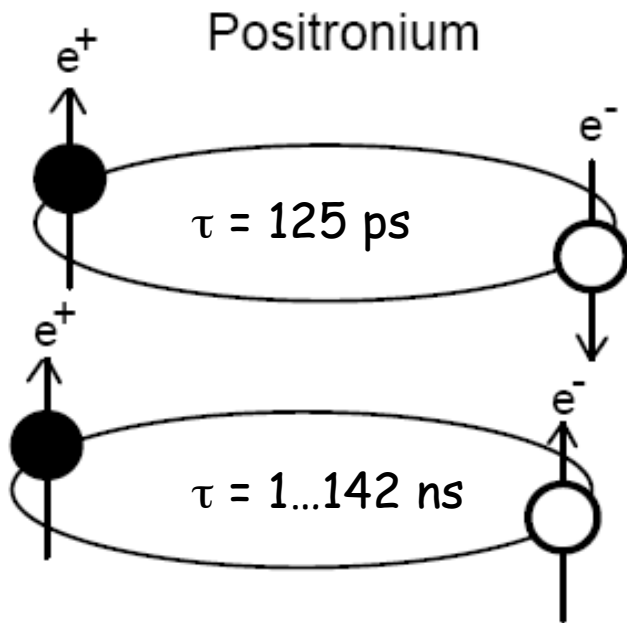
Principles of PALS: ortho-Positronium

In materials without free electrons Positronium may be formed (Polymers, glass, liquids, gases).



Pick-off annihilation

positrons form Ps

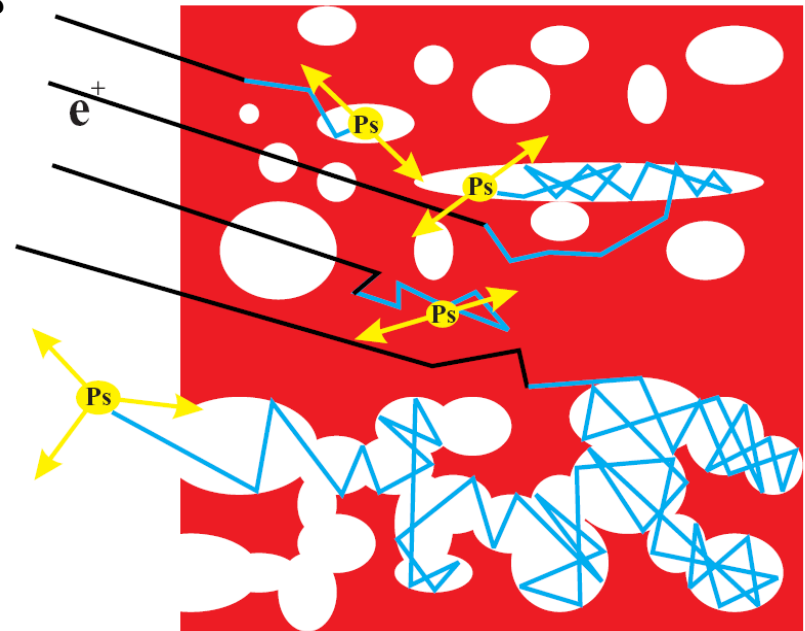


para-Ps
 1S_0

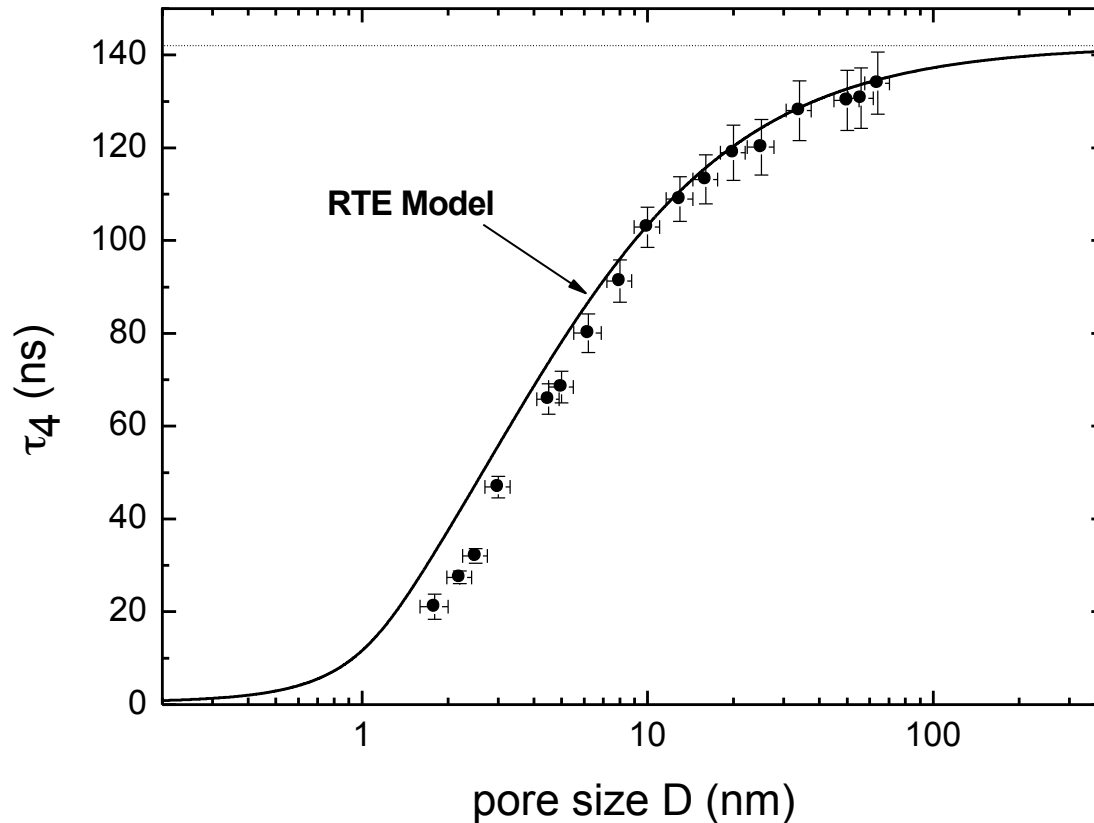
ortho-Ps
 3S_1

pick-off annihilation:

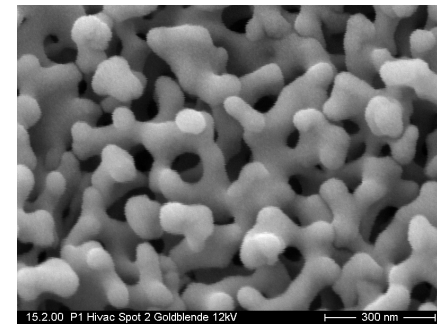
- o-Ps is converted to p-Ps by capturing an electron with anti-parallel spin
- happens during collisions at walls of pore
- lifetime decreases rapidly
- lifetime is function of pore size 1.5 ns to 142 ns



o-Ps lifetime τ_4 versus pore size



- we measured porous CPG glass in a broad pore size range



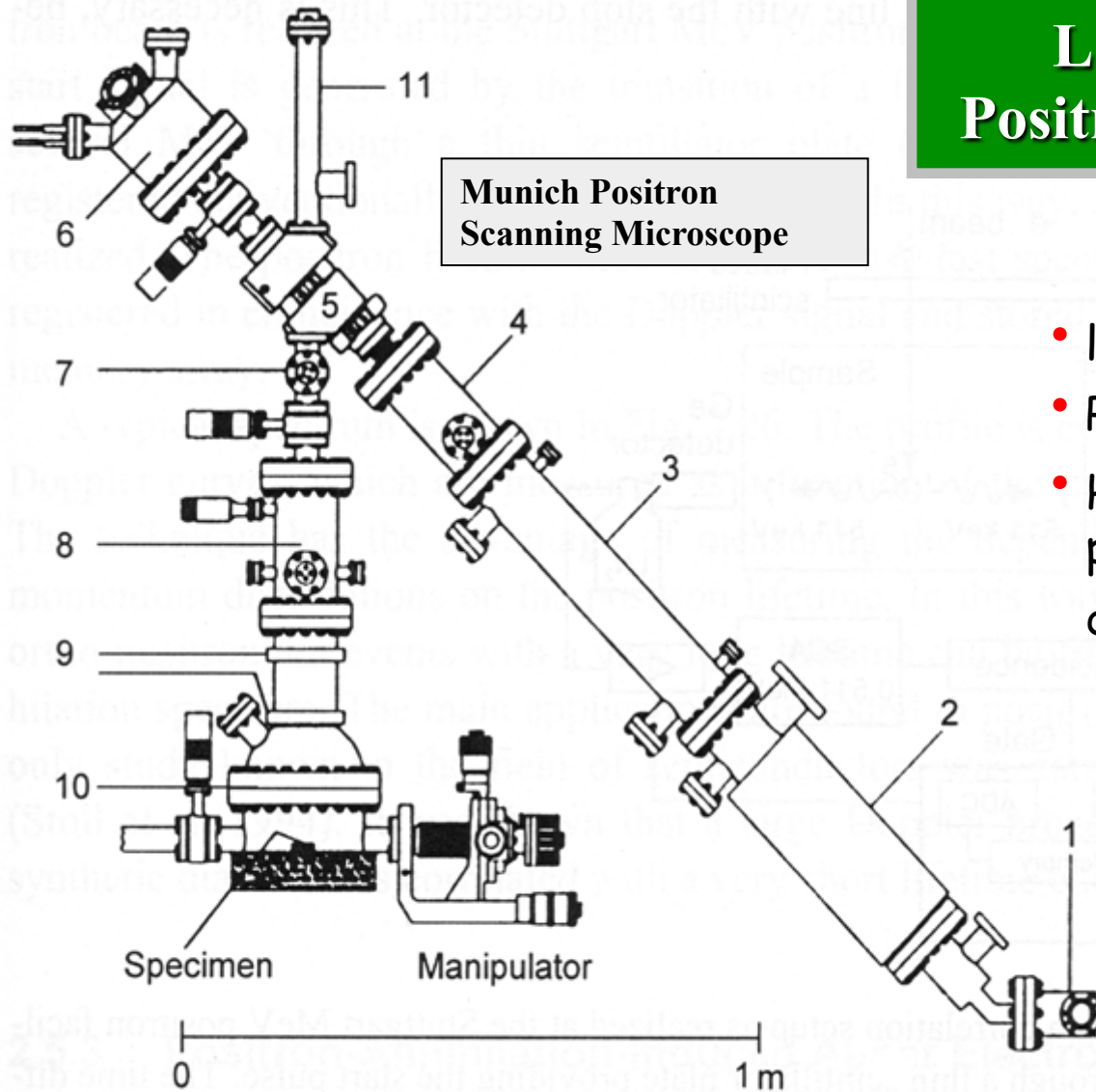
- given pore size obtained by N_2 -adsorption and/or mercury intrusion technique
- for $T=300$ K fair agreement to the RTE model for large pores

RTE model: D. W. Gidley, T. L. Dull, W. E. Frieze, J. N. Sun, A. F. Yee, *J. Phys. Chem. B* 2001, 105, 4657.



Lateral Resolution with Positron-Scanning-Microscope

Munich Positron Scanning Microscope



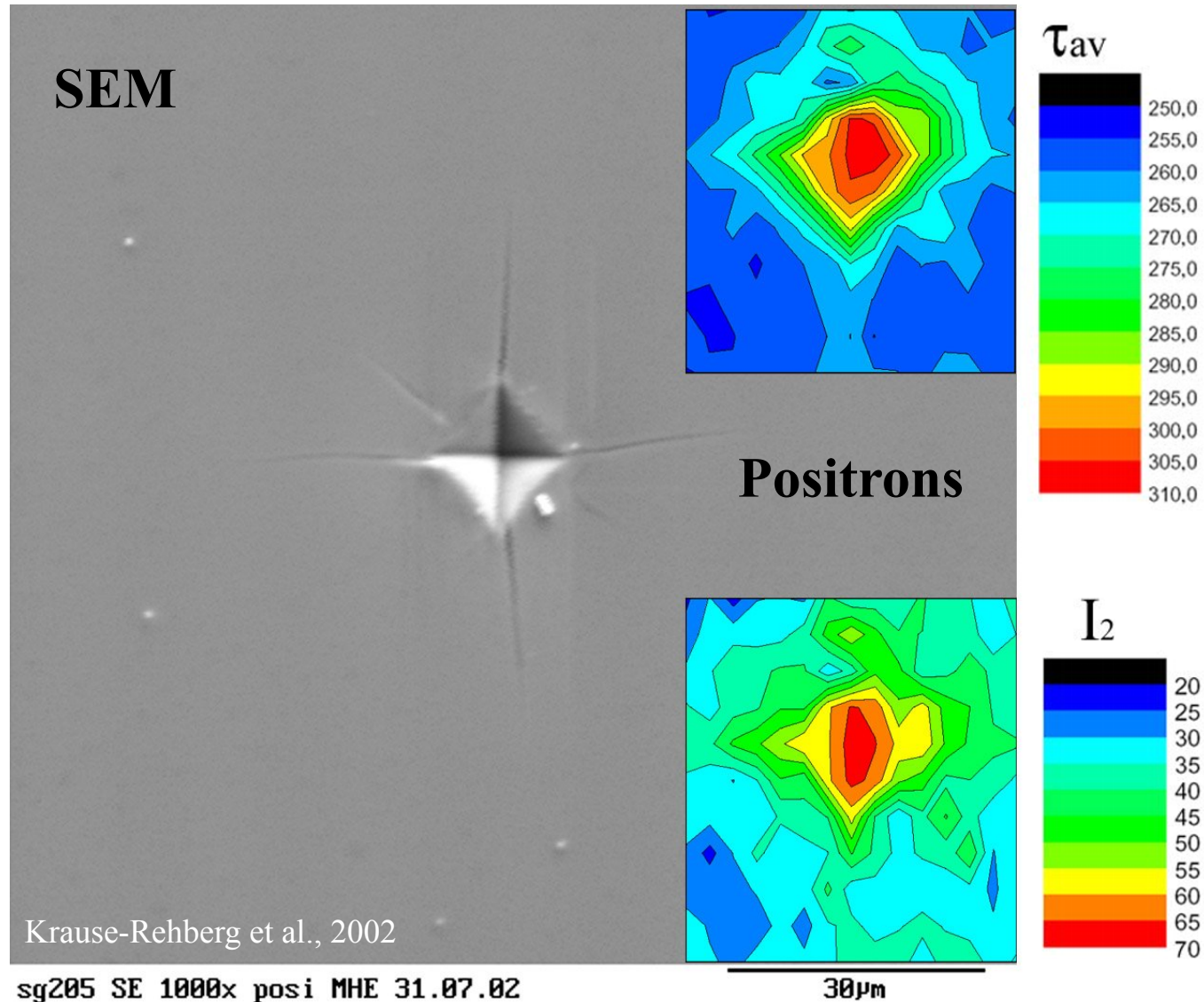
- lateral resolution $2 \mu\text{m}$
- Positron lifetime spectroscopy
- However lateral resolution principally limited by positron diffusion ($L_+ \approx 100\text{nm}$)

W. Triftshäuser et al., NIM B 130 (1997) 265

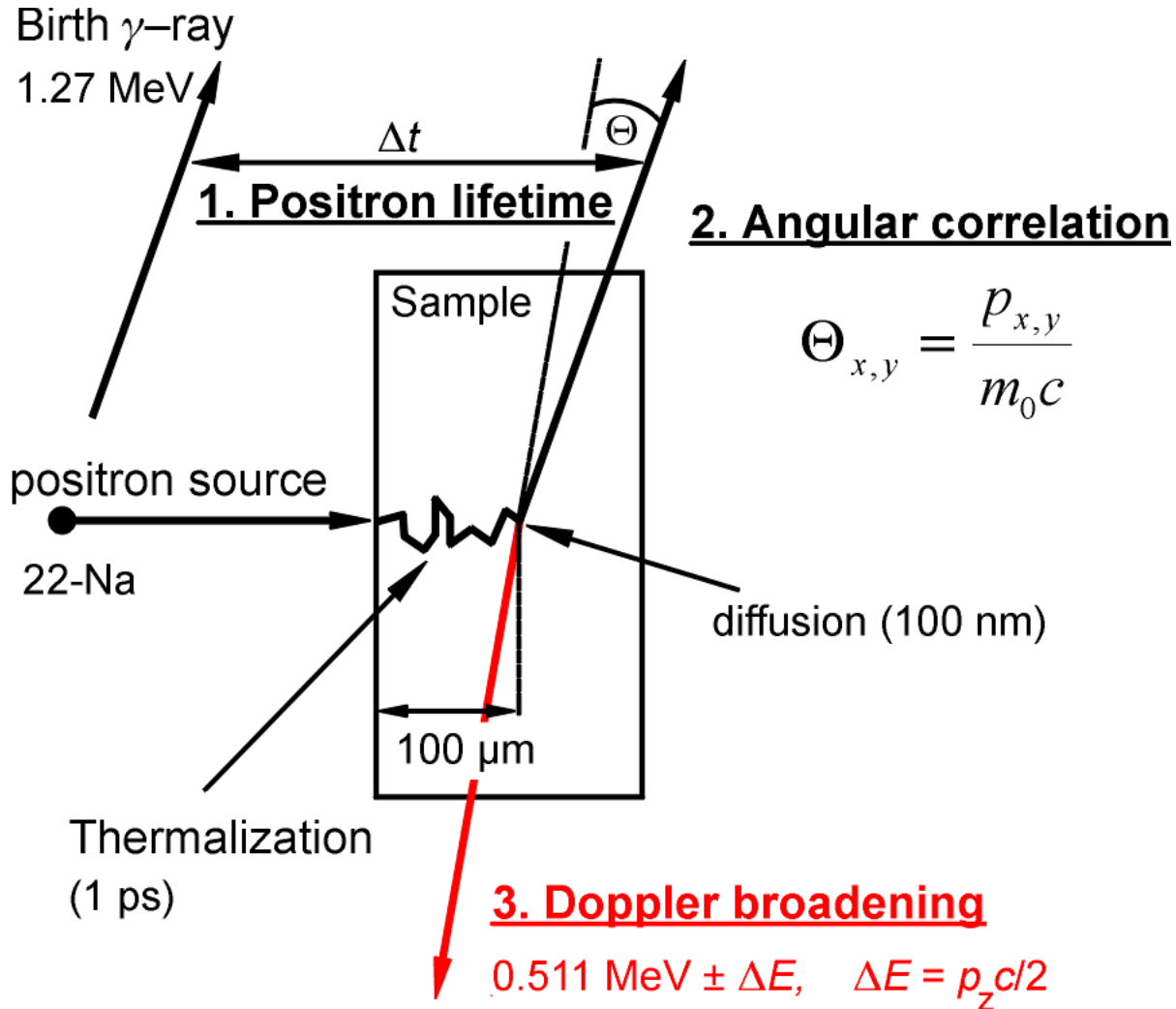


Microhardness indentation in GaAs

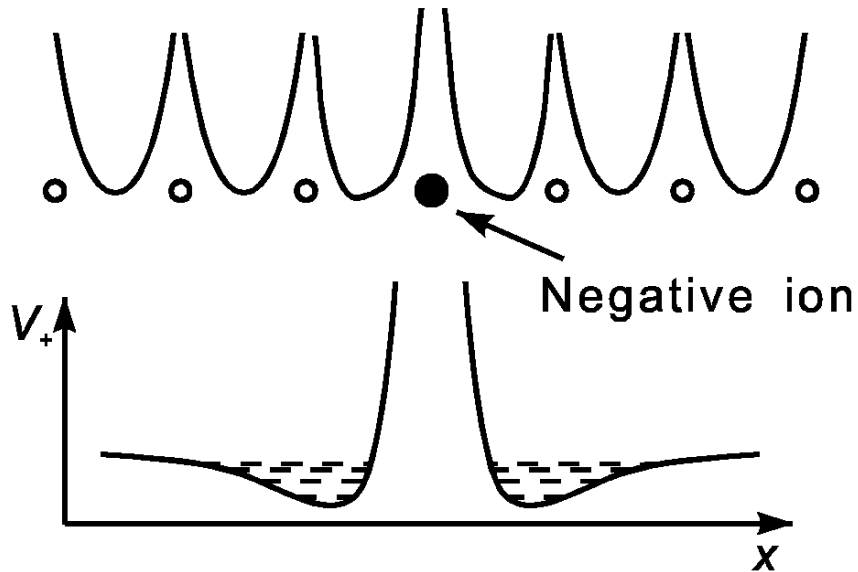
- Comparison of SEM and Munich Positron Scanning Microscope
- problem here at the moment: intensity
- hope: strong positron source at FRM-II Garching or EPOS project in Rossendorf



Three Methods of Positron Annihilation



Negative ions act as shallow positron traps

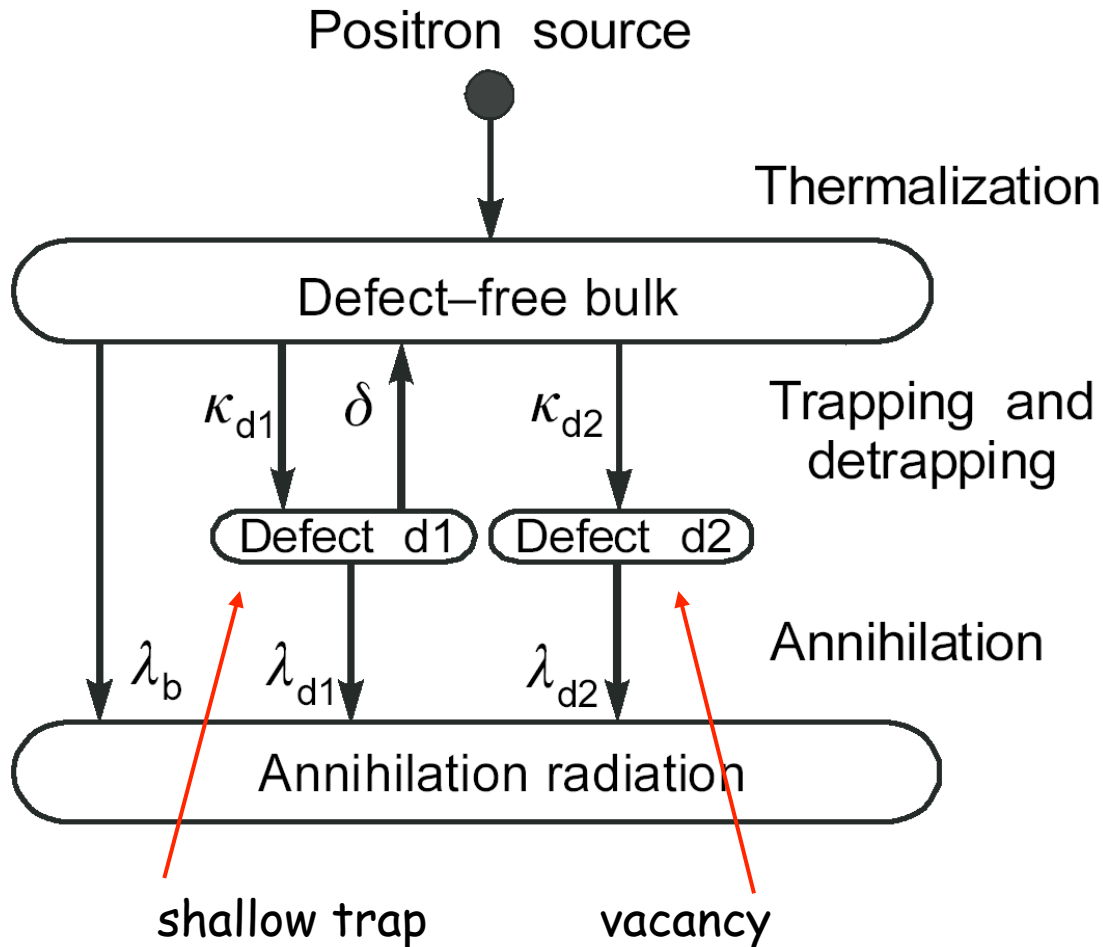


- at low T: negatively charged defects without open volume may trap positrons
- “shallow” due to small positron binding energy
- annihilation parameters close to bulk parameters
- acceptor-type impurities, dopants, negative antisite defects
- thermally stimulated detrapping can be described by:

$$\delta = \frac{\kappa}{\rho_{st}} \left(\frac{m^* k_B T}{2\pi\hbar^2} \right)^{3/2} \exp\left(-\frac{E_{st}}{k_B T} \right)$$

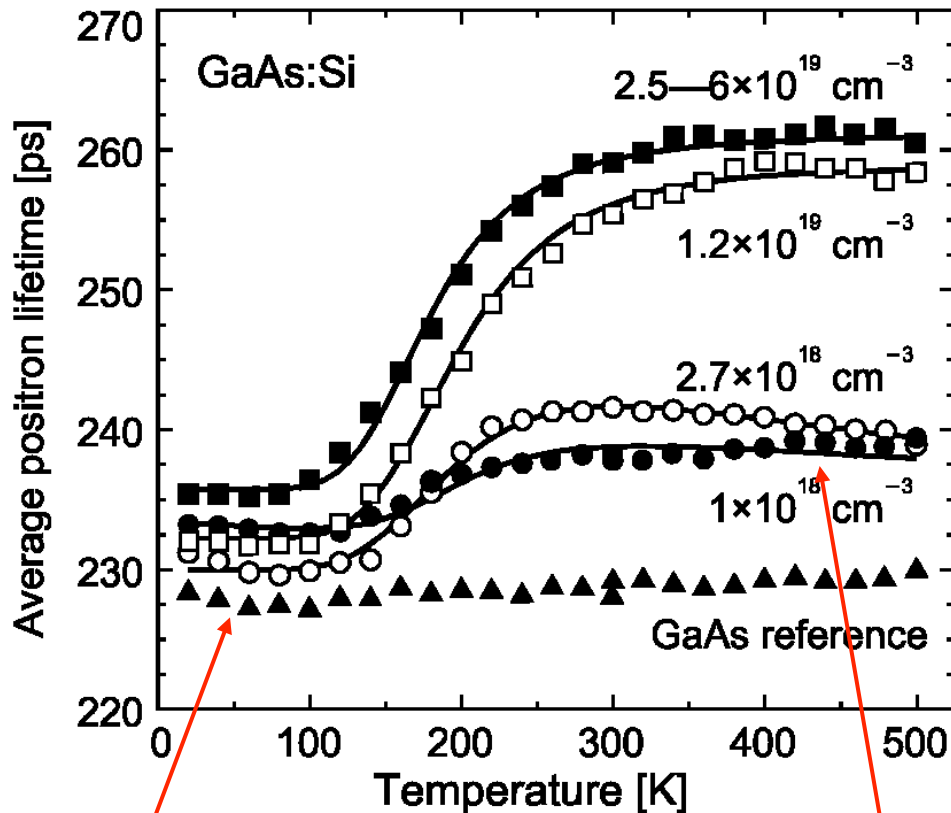
Saarinen et al., 1989

Shallow positron traps



- positron trapping model gets more complex
- however: trapping at shallow traps can be avoided at high temperatures

Effect of shallow positron traps



- temperature dependence is characterized by competing trapping by vacancies and shallow traps
- in *GaAs:Si* we observe $V_{Ga}-Si_{Ga}$ complexes at high temperatures
- and Si_{Ga}^- donors at low T in addition (shallow traps)

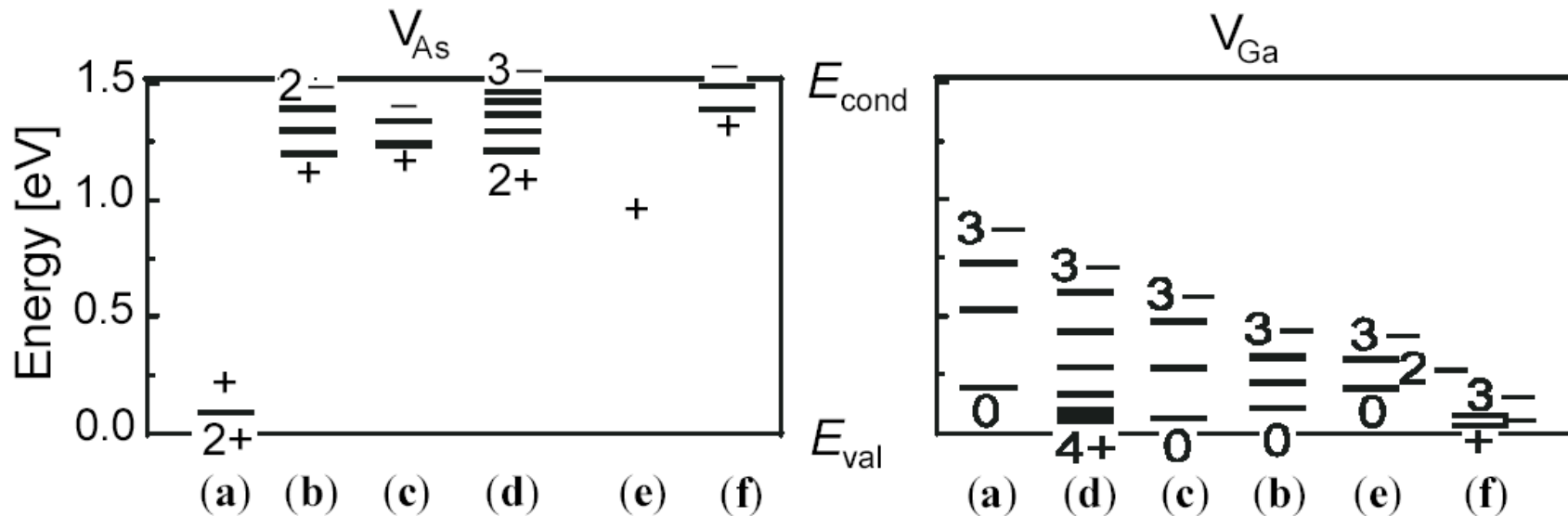
competing trapping centres at low T
shallow positron traps (Si_{Ga}^-)

trapping by vacancies
at elevated temperatures ($V_{Ga}-Si_{Ga}$)



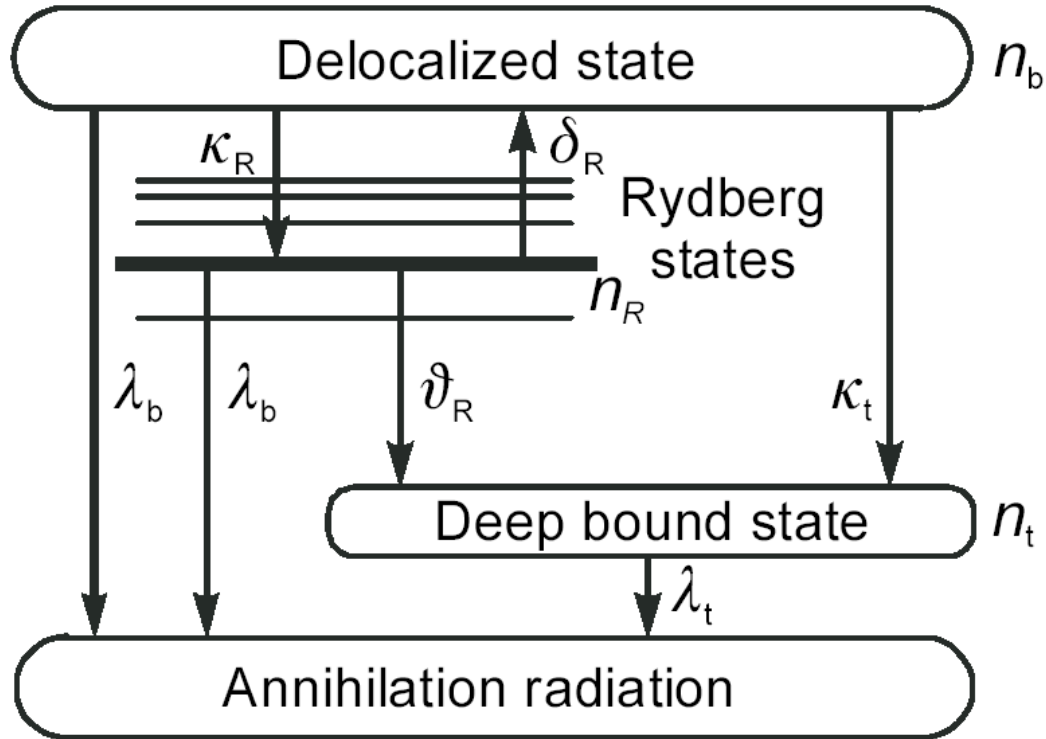
Theoretical calculation of vacancy levels in GaAs

- Theoretical description not simple
- relaxation of vacancy possible → Jahn-Teller distortion / negative-U effect



Ionization levels of arsenic vacancies, gallium vacancies, and antisites according to theoretical calculations of (a) Baraff and Schlüter (1985a), (b) Puska (1989a), (c) Jansen and Sankey (1989), (d) Xu and Lindefelt (1990), (e) Zhang and Northrup (1991), and (f) Seong and Lewis (1995), (g) Zhang and Chadi (1990), (h) Pöykkö et al. (1997). E_{val} and E_{cond} are the edges of the valence and the conduction band, respectively.

Positron trapping by negative vacancies



- trapping process can be described quantitatively by trapping model
- Coulomb potential leads to Rydberg states
- from there: positrons may re-escape by thermal stimulation
- once in the deep state: positron is captured until annihilation
- detrapping is strongly temperature dependent

$$\delta_R = \frac{\kappa_R}{\rho_v} \left(\frac{m^* k_B T}{2\pi \hbar^2} \right)^{3/2} \exp\left(-\frac{E_R}{k_B T} \right)$$

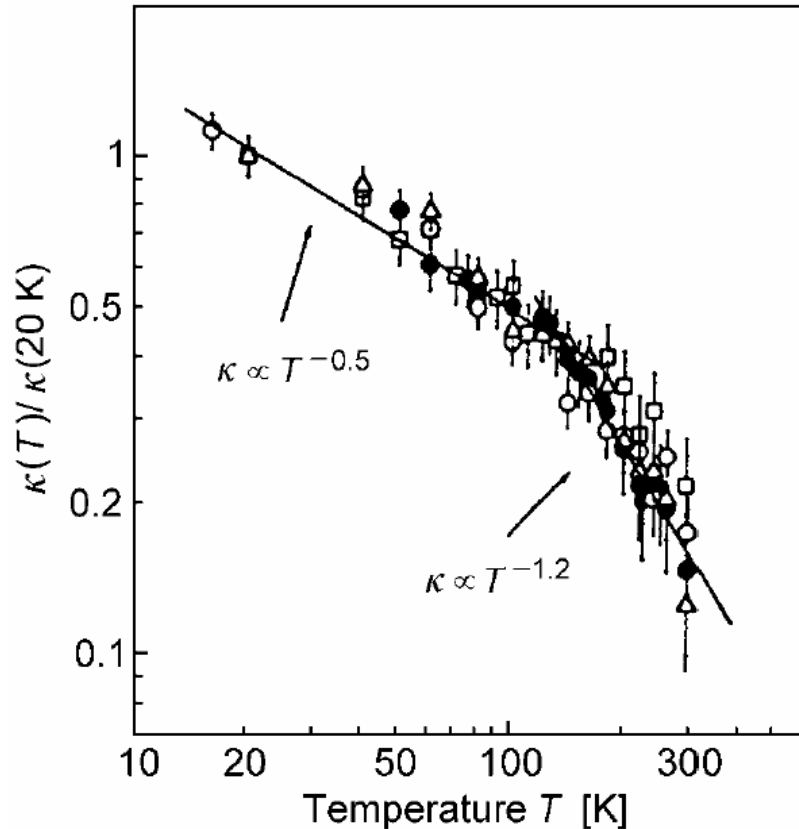
E_R binding energy of positron in Rydberg state

ρ_v vacancy density

Manninen, Nieminen, 1981



Negative vacancies show temperature-dependent positron trapping



positron trapping in negatively charged
Ga vacancies in Si-GaAs

- temperature dependence of positron trapping is rather complex

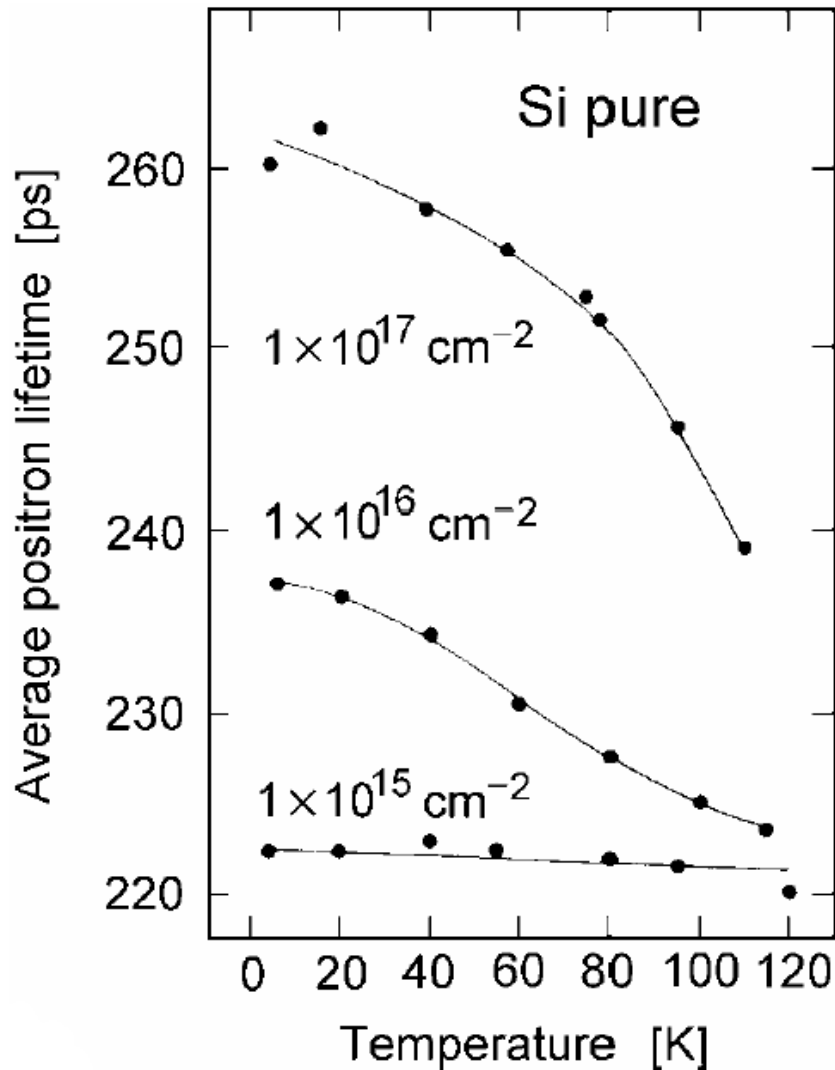
$$\kappa = \frac{\vartheta_{\text{R}} \rho_{\text{v}} \kappa_{\text{R0}} T^{-1/2}}{\vartheta_{\text{R}} \rho_{\text{v}} + \kappa_{\text{R0}} \left(\frac{m^* k_{\text{B}}}{2\pi \hbar^2} \right)^{3/2} T \exp\left(-\frac{E_{\text{R}}}{k_{\text{B}} T} \right)}$$

- low temperature: $\sim T^{-0.5}$ due to diffusion limitation in Rydberg states
- higher T: stronger temperature dependence due to thermal detrapping from Rydberg state

Le Berre et al., 1995



Temperature-dependent positron trapping



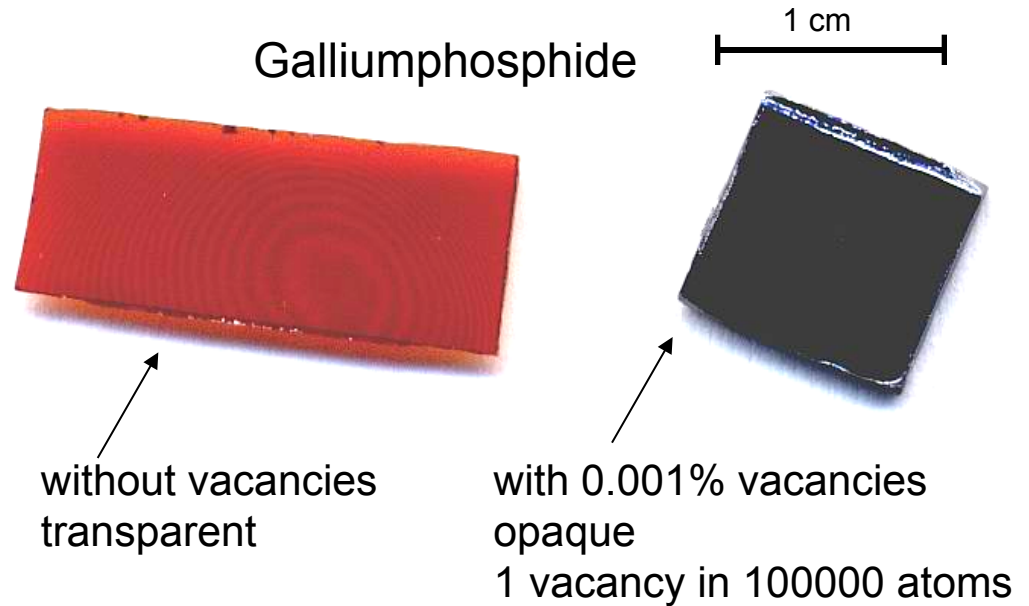
- temperature dependence of positron trapping can be used to determine the charge state of vacancies
- trapping to positive vacancies possible at elevated T
- however: has never been observed
- example: Positron trapping in e-irradiated Si
- trapping by negatively charged divacancies

(Mäkinen et al. 1989)



Point defects determine properties of materials

- Point defects determine electronic and optical properties
- electric conductivity strongly influenced
- Doping of semiconductors (n-, p-Si)



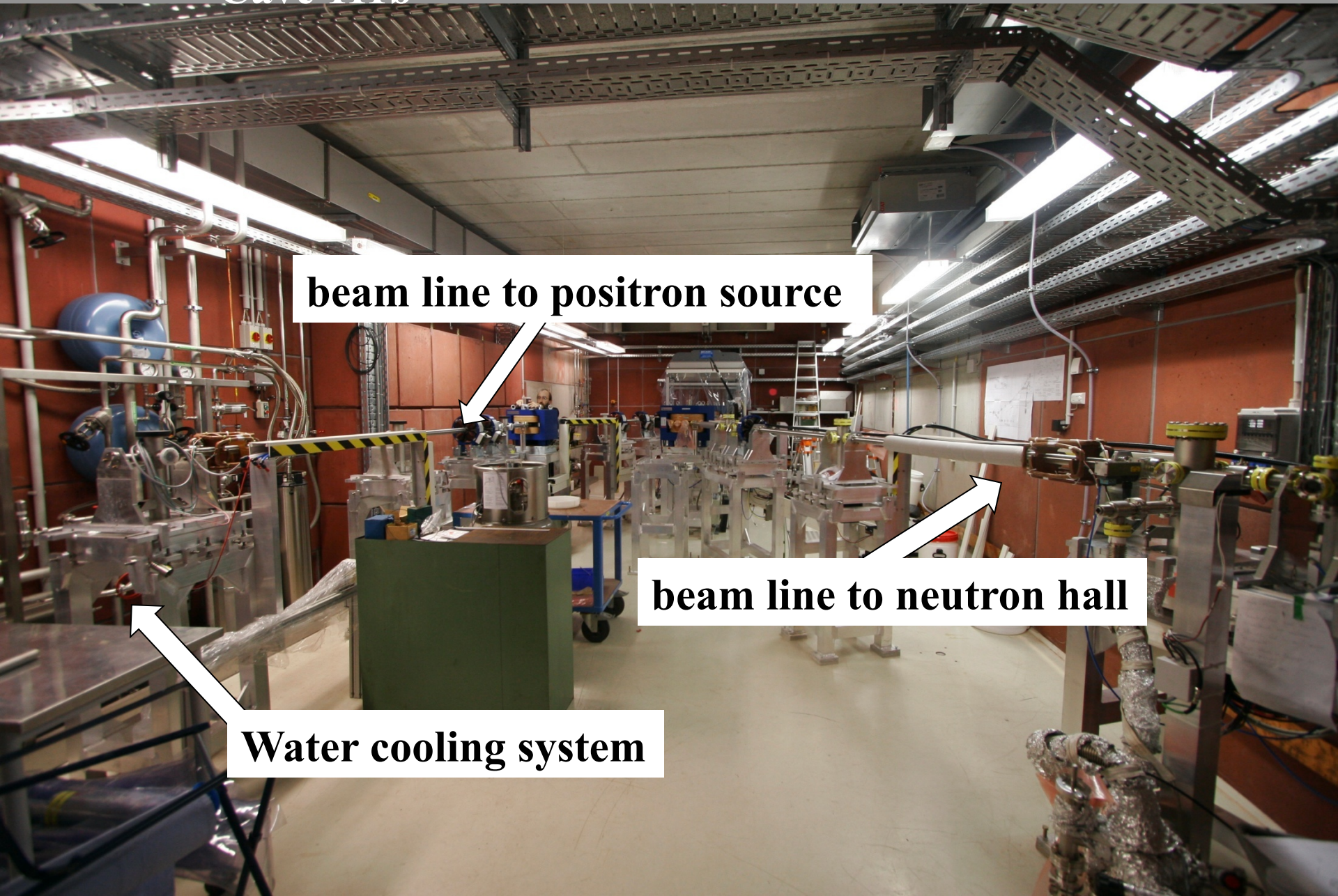
- Point defects are generated by irradiation (e.g. cosmic rays), by plastic deformation or by diffusion, ...
- Metals in high radiation environment -> formation of voids -> embrittlement
- -> Properties of vacancies and other point defects must be known
- Analytical tools are needed to characterize point defects

Cave 111b

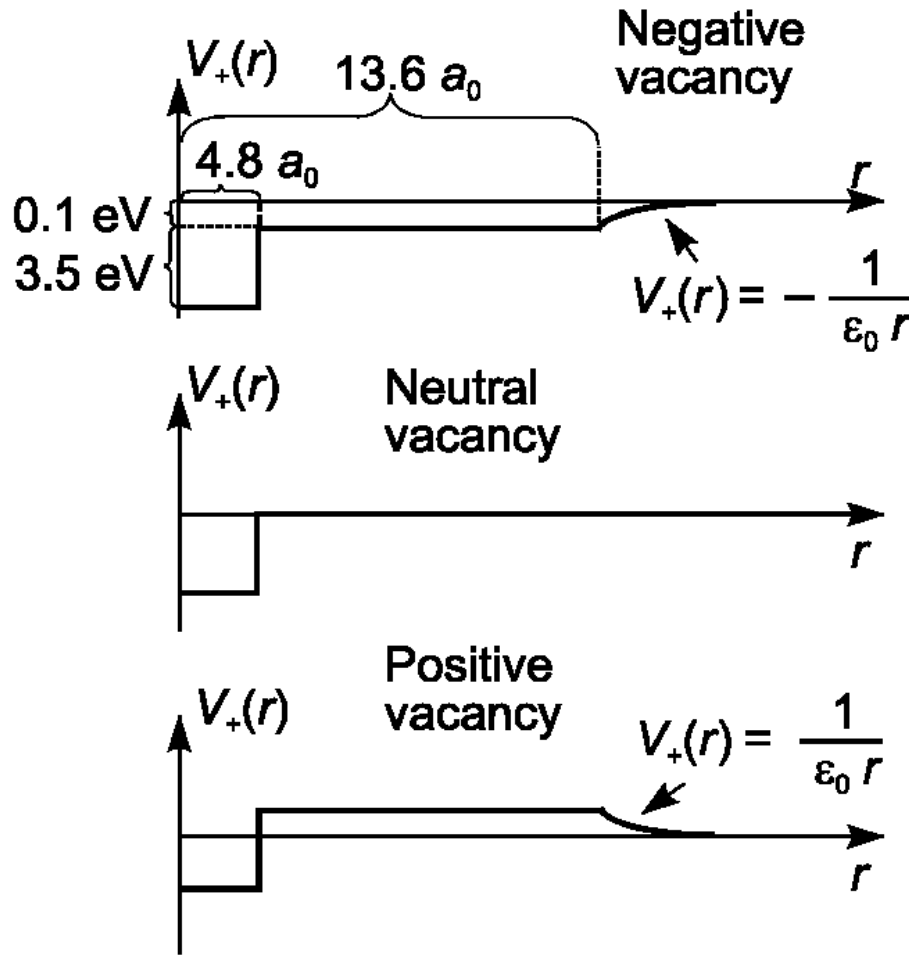
beam line to positron source

beam line to neutron hall

Water cooling system



Vacancies may be charged



Puska et al. 1990

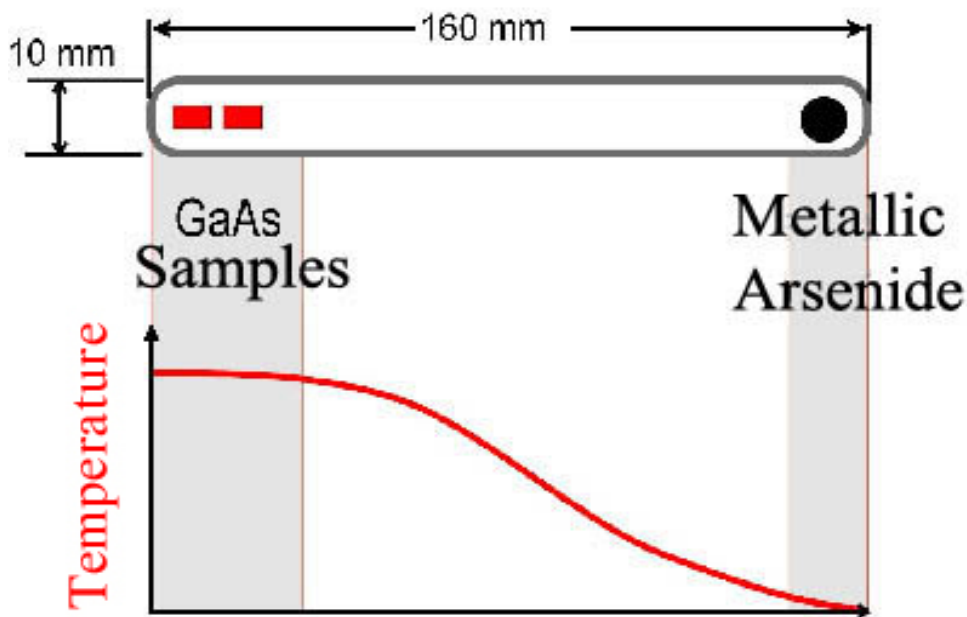
For a negative vacancy:

- Coulomb potential is rather extended but weak
- it supports trapping only at low temperatures
- at higher temperatures: detrapping dominates and vacancy behaves like a vacancy in a metal or a neutral vacancy

Positive vacancies repel positrons

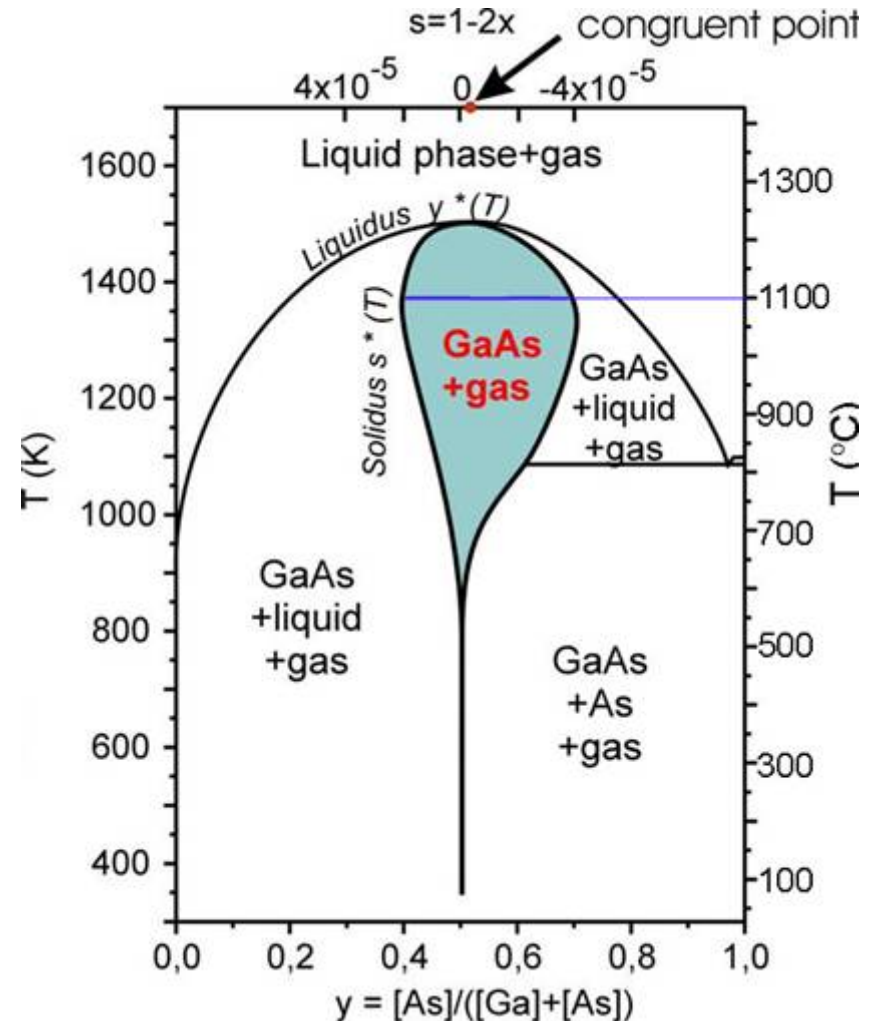
GaAs: annealing under defined As-partial pressure

- two-zone-furnace: Control of sample temperature **and** As partial pressure allows to navigate freely in phase diagram (existence area of compound)



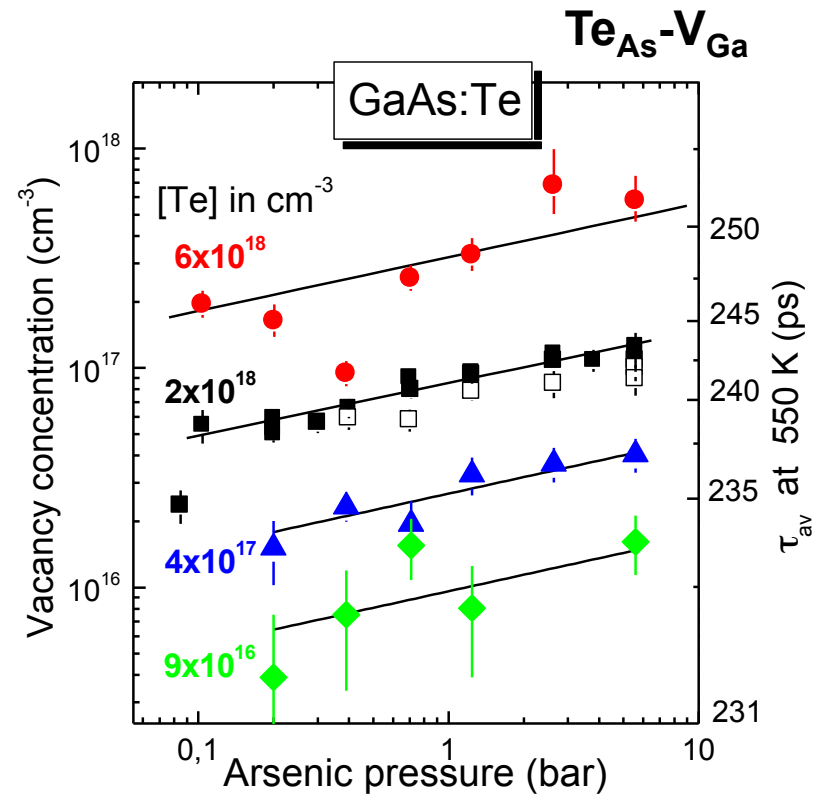
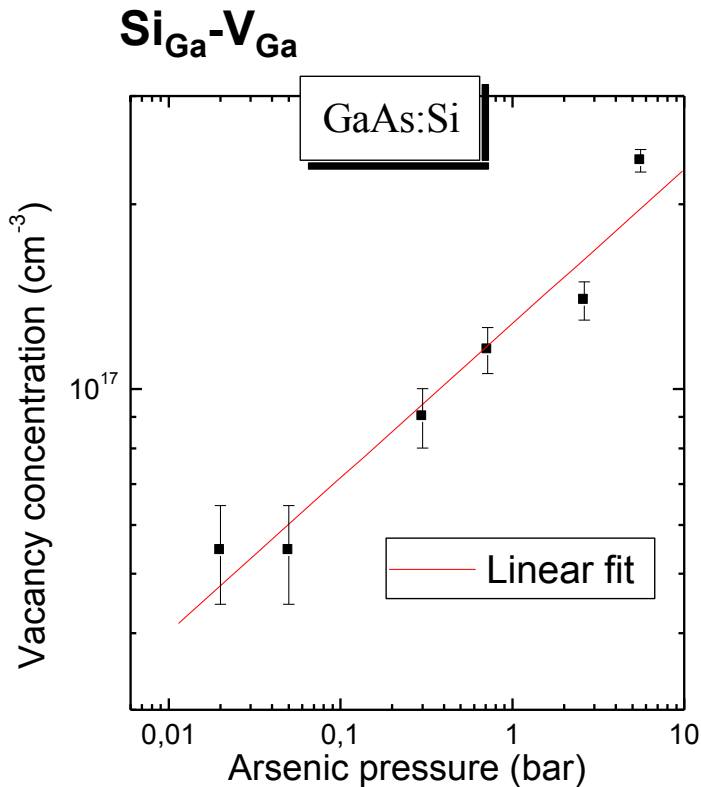
$T_{\text{sample}}: 1100^{\circ}\text{C}$

T_{As} : determines As-partial pressure

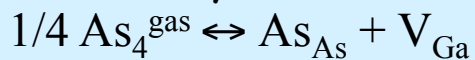


H. Wenzl et al., J. Cryst. Growth **109**, 191 (1991).

GaAs: Annealing under defined As pressure



Thermodynamic reaction:



Mass action law:

$$[\text{V}_{\text{Ga}}] = K_{\text{VG}} \times p_{\text{As}}^{1/4}$$

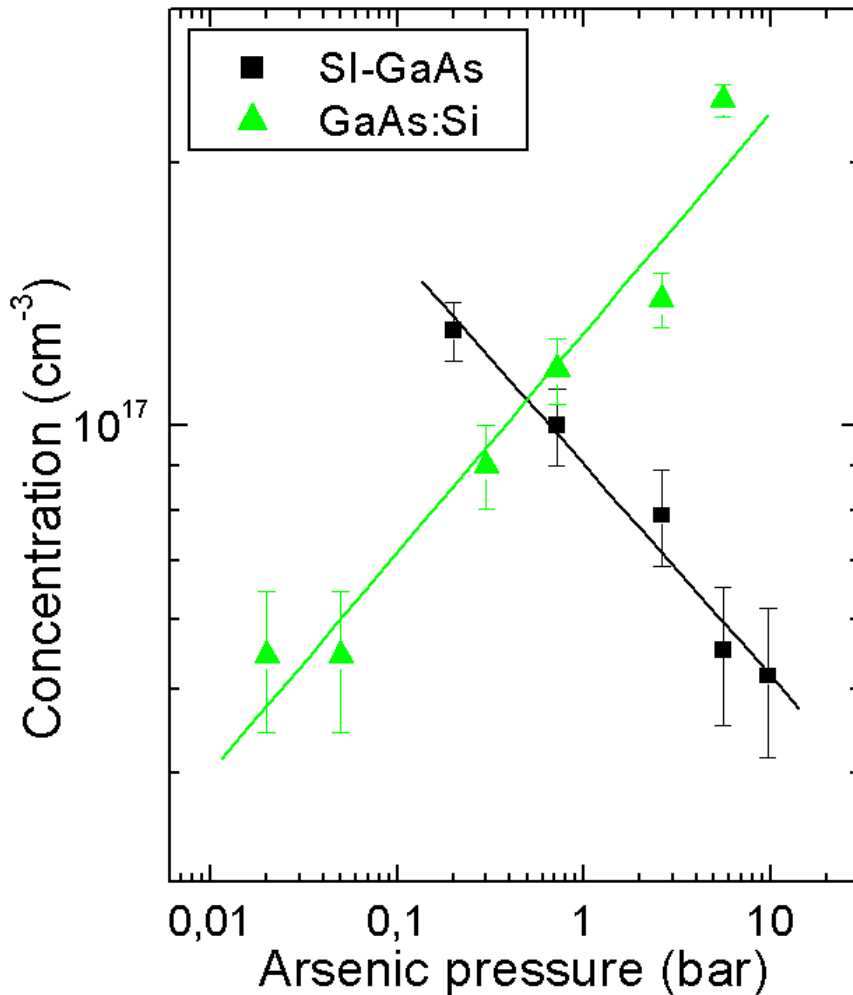
*J. Gebauer et al.,
Physica B 273-274, 705 (1999)*

Fit: $[\text{V}_{\text{Ga}}\text{-Dopant}] \sim p_{\text{As}}^n$

→ $n = 1/4$

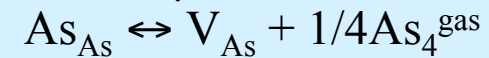


Comparison of doped and undoped GaAs



Bondarenko et al., 2003

Thermodynamic reaction:



Mass action law:

$$[\text{V}_{\text{As}}] = K_{\text{VAs}} \times p_{\text{As}}^{-1/4}$$

Fit: $[\text{V-complex}] \sim p_{\text{As}}^n$

$$\rightarrow n = -1/4$$

undoped GaAs: As vacancy

